Applied Catalysis B: Environmental 343 (2024) 123479

Contents lists available at ScienceDirect

Applied Catalysis B: Environmental

journal homepage: www.elsevier.com/locate/apcatb

Selective catalytic reduction of NO_x by NH_3 over Cu-AEI zeolite catalyst: Current status and future perspectives

Yao Wang [a,b], Junhua Li [c], Zhiming Liu [a,b,*]

[a] State Key Laboratory of Chemical Resource Engineering, Beijing University of Chemical Technology, Beijing 100029, China
[b] College of Chemical Engineering, Beijing University of Chemical Technology, Beijing 100029, China
[c] State Key Joint Laboratory of Environment Simulation and Pollution Control, School of Environment, Tsinghua University, Beijing 100084, China

ARTICLE INFO

Keywords:
NH_3-SCR
Nitrogen oxides
AEI zeolites
Cu-SSZ-39
Cu-SAPO-18

ABSTRACT

Cu-exchanged small-pore SSZ-39 and SAPO-18 (Cu-AEI) zeolite catalysts have attracted more and more attention due to the high NH_3-SCR performance and remarkable hydrothermal stability, which are crucial for the control of NO_x from the diesel exhaust. This paper comprehensively reviews the research progress on Cu-AEI zeolites for NH_3-SCR of NO_x, encompassing the NH_3-SCR reaction mechanism, hydrothermal aging mechanism, chemical poisoning mechanism, multi-route synthesis method, and performance optimization method. Our objective is to provide a fundamental understanding of the NH_3-SCR reaction over Cu-AEI zeolite catalysts and highlight the relationship between the structure and the catalytic performance, which would shed light on the design of more highly active and durable Cu-AEI zeolite catalyst for the NH_3-SCR of NO_x. Finally, the challenges and prospects for Cu-exchanged small-pore zeolites have been proposed, which would promote the practical application of these catalysts to meet the strict emission regulations in the future.

1. Introduction

Nitrogen oxides (NO_x) emitted from the diesel vehicle and stationary sources can cause serious environmental issues, such as acid rain, greenhouse effect, and photochemical smog [1]. Selective catalytic reduction of NO_x with NH_3 (NH_3-SCR) is one of the most effective technologies for the control of NO_x from diesel exhaust, and the catalyst plays a key role for this method [2]. For the diesel exhaust, the temperature can vary in a wide temperature range, such as the high temperatures (>650 °C) caused by the regeneration of the diesel particulate filer (DPF) and the low temperatures (<200 °C) at the cold start stage. Additionally, it contains different components, such as H_2O, SO_2, phosphorus, alkali and alkaline earth metals, and the products formed due to the incomplete fuel combustion, which can poison the catalyst. Therefore, the catalyst should have a broad activity temperature window, excellent hydrothermal stability, and resistance against the toxic substances. Commercial V_2O_5-based catalyst is not applicable due to their poor hydrothermal stability, narrow activity temperature window as well as the toxicity of vanadium [3]. As a result, vanadium-free NH_3-SCR catalysts with high efficiency, excellent hydrothermal stability and chemical poisoning resistance have been intensively explored.

In recent decades, zeolite-based catalysts with unique pore structures and excellent catalytic performance have attracted increasing attention and application in petrochemical, energy, and environmental fields [4–6]. Zeolite is divided into small-pore zeolite with 8-membered rings, medium-pore zeolite with 10-membered rings, large-pore zeolite with 12-membered rings, and extra-large-pore zeolite with more than 12-membered rings. Small-pore zeolite can effectively limit the diffusion of framework dealumination products and HC compounds within the pore channels of zeolite due to their pore size, resulting in high hydrothermal stability and tolerance to HC poisoning. In addition, the acid sites in zeolites can be regulated by different methods to promote the reaction. Metal-exchanged small-pore zeolites are the most effective catalysts for the removal of NO_x from diesel exhaust. Cu-CHA (Cu-SSZ-13 and Cu-SAPO-34) catalysts have been intensively studied. Kwak et al. [7] first reported the catalytic performance of Cu-SSZ-13 in the NH_3-SCR reaction, and found Cu-SSZ-13 catalyst showed higher activity than Cu-BEA and Cu-ZSM-5 zeolites. Subsequently, Fickel et al. [8] found that Cu-SAPO-34 and Cu-SSZ-13 exhibited similar SCR performance with the same CHA structure. Cu-CHA zeolites are superior to medium and large pore zeolites due to their demonstrated activity and hydrothermal stability in the NH_3-SCR reaction [7,9,10]. Cu-exchanged SSZ-13 and SAPO-34 (Cu-CHA) catalysts have been applied commercially for the purification of the diesel exhaust. However, the

* Corresponding author at: State Key Laboratory of Chemical Resource Engineering, Beijing University of Chemical Technology, Beijing 100029, China.
E-mail address: liuzm@mail.buct.edu.cn (Z. Liu).

https://doi.org/10.1016/j.apcatb.2023.123479
Received 10 August 2023; Received in revised form 14 October 2023; Accepted 6 November 2023
Available online 7 November 2023

hydrothermal stability of Cu-SSZ-13 catalyst still needs to be improved. For example, hydrothermal aging at 850 °C inevitably leads to a significant decrease in the surface area and pore volume of the zeolite, thus the SCR activity is decreased dramatically [10–12].

As the emission regulation becomes more and more stringent around the world, it is desirable to develop other zeolites with high catalytic activity and hydrothermal stability. Hong et al.[13] first applied Cu-LTA zeolite for the NH_3-SCR reaction, and found this catalyst is of exceptional hydrothermal stability, with high activity even after exposure to the hydrothermal aging at 900 °C. Subsequently, Lin et al.[14] also reported that Cu-LTA catalyst possessed excellent hydrothermal stability by adjusting the Cu loading. Although Cu-LTA catalyst demonstrate outstanding activity and good hydrothermal stability, the synthesis process is complicated and more simple synthesis method needs to be developed.

AEI zeolite has attracted more and more attention because it is of the exact same topology as the primary unit of CHA zeolite (shown in Fig. 1). These catalysts consist of larger interconnected cages bound by 8-membered ring pores and double 6-membered rings. Due to the structural similarities of these two types of zeolites, Cu-AEI catalyst has been intensively studied for the NH_3-SCR reaction and demonstrated to be a potential candidate for the control of NO_x.

To date, some reviews have been reported for the Cu-CHA catalysts [15–20]. However, little review on Cu-AEI catalyst has been published. This review focuses on the recent progress on Cu-AEI catalyst for the NH_3-SCR of NO_x. In this review, the reaction mechanism will be described first, then the method for synthesizing and regulating the structure of the zeolite, the hydrothermal stability, the low-temperature SCR activity, and the catalyst deactivation will be discussed (Fig. 2). Furthermore, the challenges and opportunities for this type of catalyst as well as the future research perspectives for the NH_3-SCR of NO_x are proposed. This review would help researchers extend the understanding of the fundamental scientific principles in the catalytic removal of NO_x over Cu-AEI catalyst, thus speeding up their industrial application to meet the tightening emission regulations.

2. Mechanism of NH_3-SCR reaction on Cu-AEI

NH_3-SCR of NO_x can proceed by the standard SCR reaction [Eq. (1)] or the fast SCR reaction(when $NO/NO_2 = 1$) [Eq. (2)].

$$4NH_3 + 4NO + O_2 = 4\ N_2 + 6\ H_2O \quad (1)$$

$$2NH_3 + NO + NO_2 = 2\ N_2 + 3\ H_2O \quad (2)$$

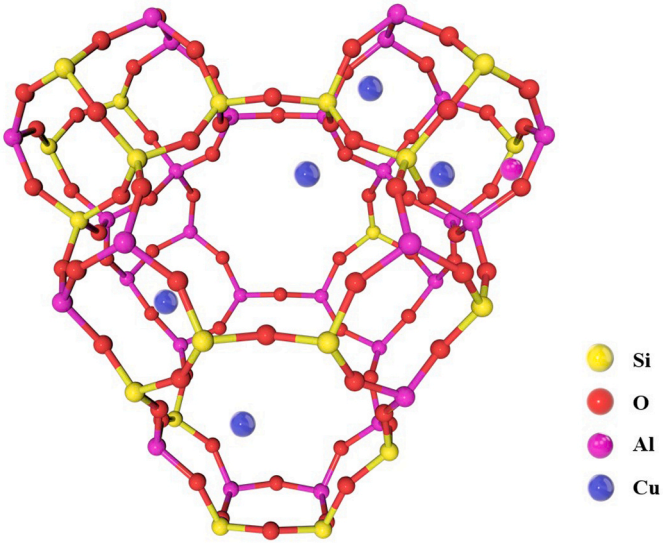

Fig. 1. Structure of Cu-AEI catalyst.

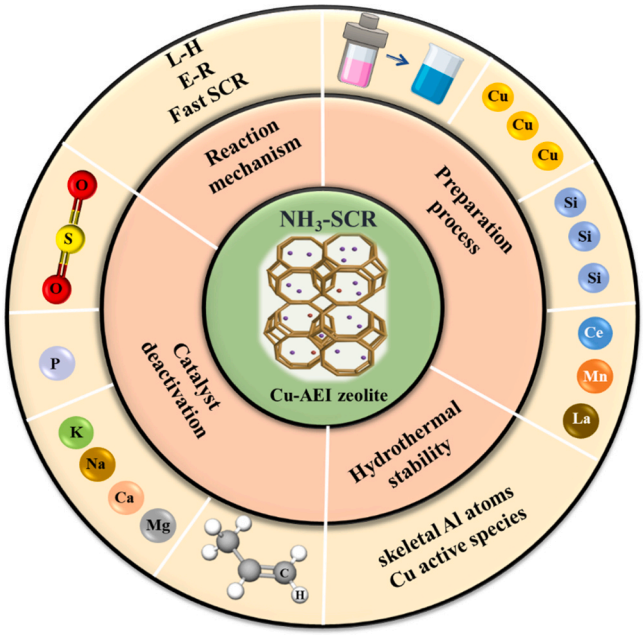

Fig. 2. Scheme of this review.

The NH_3-SCR reaction mechanism can be divided into two types: "Langmuir-Hinshelwood (L-H)" and "Eley-Rideal (E-R)" mechanisms, as illustrated in Fig. 3. For the "E-R" mechanism, NH_3 molecules are adsorbed and activated on the Brønsted and Lewis acid sites to form NH_4^+ ions or coordinated NH_3, which subsequently react with gaseous NO to form active intermediate NH_2-NO/NH_3-NO, and then decomposes into N_2 and H_2O. For the "L-H" mechanism, the adsorbed NH_3 species can form NH_4^+ species, and NO is oxidized on the high-valent redox site to form active bidentate nitrate/monodentate nitrite/bridged nitrate, then these intermediates react with NH_4^+ to generate NH_4-NO_2/NH_4-NO_3, which subsequently decompose into N_2 and H_2O.

2.1. Reaction mechanism on Cu-SSZ-39 catalyst

Over the Cu-SSZ-39 catalyst, Fu et al.[21] found the NH_3-SCR reaction follows both the "E-R" and "L-H" mechanisms at low temperatures. As shown in Scheme 1, two adjacent Cu^{2+} ions are located in large cages near two adjacent d6r units. The Cu^{2+} on the left side participates in the NH_3 reaction cycle, and the Cu^{2+} on the right side participates in the NO oxidation cycle (the commonly believed Cu^{2+}/Cu^{+} redox cycle does not exist). Both cycles form NH_4NO_3 and NH_4NO_2, which subsequently react

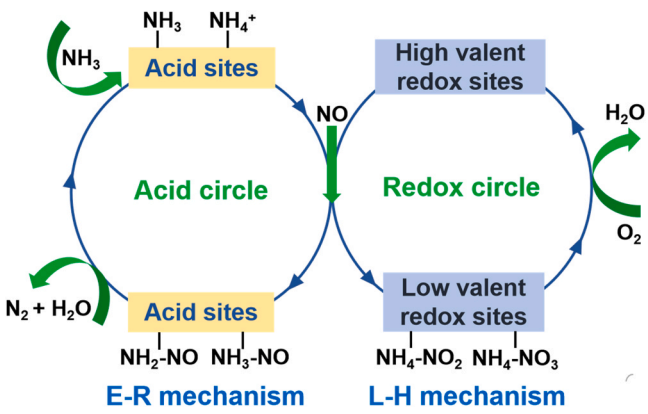

Fig. 3. A schematic diagram for the SCR reaction pathway over metal oxide and zeolite catalysts. Reprinted from [1] with permission of American Chemical Society.

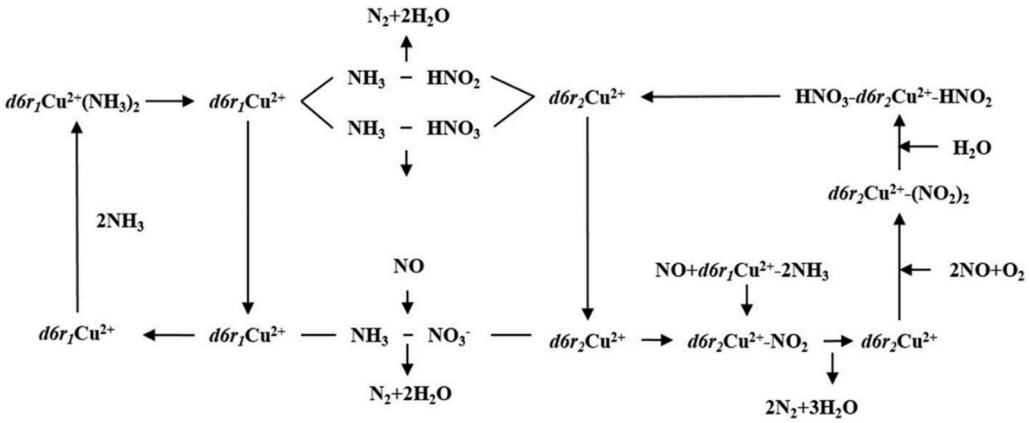

Scheme 1. The supposed reaction mechanism of NH_3-SCR on Cu/SSZ-39. Reprinted from [21] with permission of Elsevier.

with NO to form N_2 or decompose directly into N_2 and H_2O. So far, the reaction mechanism of NH_3-SCR is still widely debated due to the different catalyst components with varied redox and acidic capabilities, which result in various NH_x/NO_x active intermediates and different reaction routes.

Previous studies showed two NH_3-SCR reaction pathways: One is the "NH_4NO_2 pathway" (NO produces nitrite, which then reacts with NH_3 to produce N_2 and H_2O), and the other is the "NH_4NO_3 pathway" (NO reacts with NH_4NO_3 to yield N_2, NO_2, and H_2O). Based on the above findings, Zhu et al.[22] hold the view that the Cu-SSZ-39 catalyst followed both reaction pathways, as presented in Fig. 4. On Cu-SSZ-39, NO_2 dimerization and disproportionation reactions lead to the formation of surface nitrates (reactions 5 and 6). According to the results of Ruggeri et al.[23], it can be found that NO^+ species acts as a critical surface intermediate in the standard SCR reaction, continuously forming NO_2 or surface nitrate species. The presence of a small amount of NO^+ species on Cu-SSZ-39 was found by in-situ diffuse reflectance infrared Fourier transform spectroscopy (DRIFTS) technique. NO^+ can combine

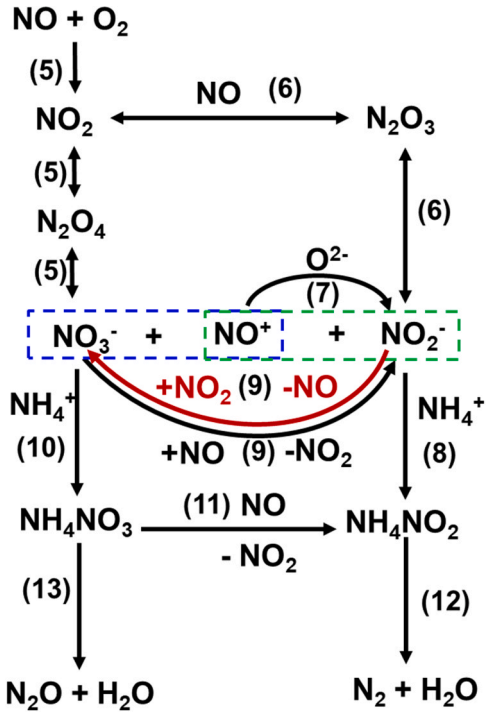

Fig. 4. Scheme of NH_3-SCR reaction pathways on Cu-SSZ-39. Reprinted from [22] with permission of American Chemical Society.

with O^{2-} to form NO_2^- (reaction 7), which subsequently reacts rapidly with NH_3 adsorbed on the Lewis acid site (reactions 8 and 12). The low number of NO^+ species on the surface of the Cu-SSZ-39 catalyst reflects its low NO oxidation ability, and hence the relatively slow standard SCR reaction occurring at low temperatures. In addition, when NO_2 was introduced to Cu-SSZ-39, the NO gas was immediately produced (reaction 9). The nitrate on the catalyst surface reacts with the pre-adsorbed NH_3 on the acid sites to form NH_4NO_3 (reaction 10), and more NH_4^+ is adsorbed than NH_3 species, representing the conversion of NH_3 on more Lewis acid sites to NH_4-NO_x. The reaction between NH_4NO_3 and NO (reactions 11 and 12) is the key step in the SCR process, and the produced NO_2 can be adsorbed and reacted with NH_3 again. Meanwhile, NH_4NO_3 was formed in the SCR reaction. And above 200 °C, NH_4NO_3 can be decomposed into N_2O and H_2O (reaction 13). In summary, the "NH_4NO_2 pathway" and the "NH_4NO_3 pathway" exist in the fast SCR and standard SCR reactions over Cu-SSZ-39 catalysts. The response of the "NH_4NO_3 pathway" is facilitated by NO_2 under fast SCR conditions.

Considering the possible differences in the reaction mechanism at different temperatures, Lin et al.[24] studied the reaction mechanism of NH_3-SCR on Cu-SSZ-39 zeolite in two different reaction temperature ranges (150–350 °C and 350–550 °C). The reaction of adsorbed ammonia with gaseous NO + O_2 was found in both reaction temperature ranges. It was accompanied by the consumption of ionic nitrate, indicating that the "L-H" and "E-R" mechanisms occurred simultaneously. Different from this report, Wang et al.[25] found that over Cu-SSZ-39 catalyst the reaction only follows the "L-H" mechanism.

The promoter not only promotes the activity, but also changes the reaction mechanism in some cases. The SCR activity of the Mn-modified Cu-SSZ-39 catalyst was unexpectedly increased after the hydrothermal treatment [23]. Both the "L-H" and "E-R" mechanisms were followed on the hydrothermally treated MnCu-SSZ-39 catalyst (see Fig. 5), and the "fast SCR" reaction occurred simultaneously. Whereas over pristine Cu-SSZ-39 catalyst, the reaction only follows the "L-H" mechanism.

2.2. Reaction mechanism on Cu-SAPO-18 catalyst

The potential intermediates and possible reaction mechanism over Cu-SAPO-18 catalyst in the NH_3-SCR reaction were proposed by Li et al. [26]. It has been reported that the coordinated NH_3 is more easily to participate in the reaction, and the Brønsted acid site mainly acts as a storage site for NH_3. The NH_3-SCR reaction path over the Cu-SAPO-18 catalyst is depicted in Fig. 6, which includes the standard SCR reaction (outside cycle) and the fast SCR reaction (inside cycle). In the overall NH_3-SCR reaction cycle, the key reaction steps are NH_3 dissociation to NH_2 and NO oxidation to NO_2. N_2 is generated through the reduction of Cu^{2+} species and the oxidation of Cu^+ species.

The doping of other metals to Cu zeolites is an effective way to improve the NH_3-SCR activity of catalyst, and the enhancement of the

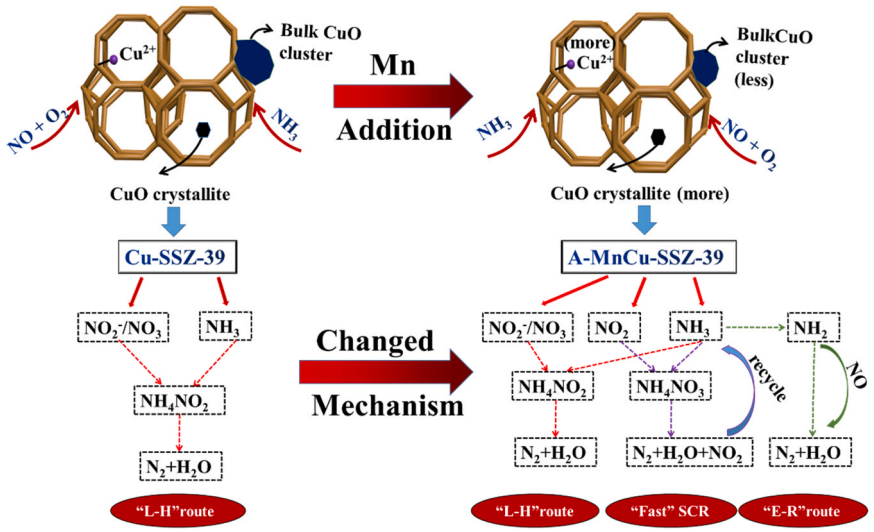

Fig. 5. Schematic diagram of NH_3-SCR reaction mechanism over Cu-SSZ-39 and MnCu-SSZ-39.

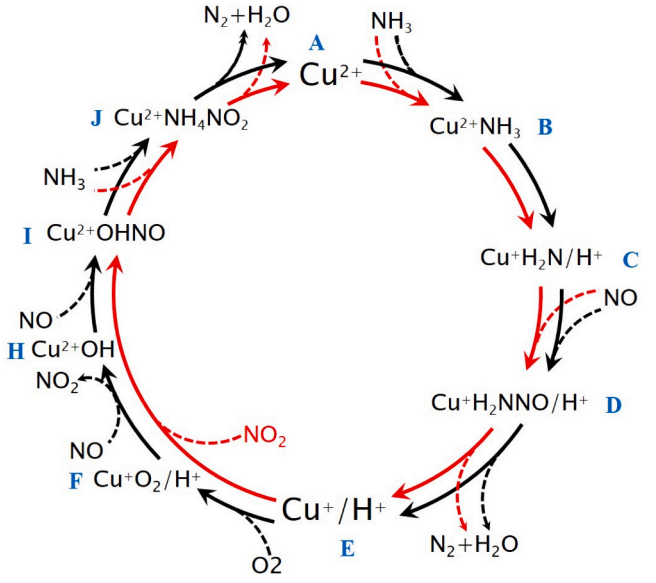

Fig. 6. Proposed NH_3-SCR reaction path over Cu-SAPO-18 catalyst. The fast SCR cycle is represented in red (inside), and the standard SCR cycle is represented in black (outside). Reprinted from [26] with permission of American Chemical Society.

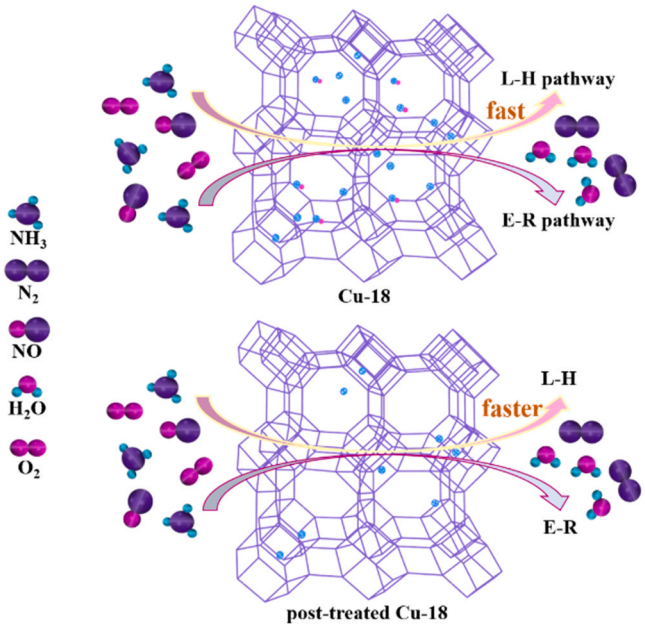

Fig. 7. Schematic diagram of NH_3-SCR reaction mechanism over Cu-18, Mn/Cu-18-III and MMn/Cu-18-III at 200 °C. Reprinted from [28] with permission of Elsevier.

NH_3-SCR performance may be accompanied by a change in the reaction mechanism. Wu et al.[27] found that the NH_3-SCR reaction over Cu-SAPO-18 and CeCu-SAPO-18 catalysts follows both "L-H" and "E-R" mechanisms. For the "L-H" mechanism, the introduction of Ce promotes the increase of Cu^{2+} content, which facilitates the adsorption and activation of NO molecules (especially the formation of NO^+, a key intermediate in the reaction process), and the occurrence of the "fast SCR" reaction further enhances the low-temperature activity. For the "E-R" mechanism, the introduction of Ce leads to the increase of Lewis acid sites in CeCu-SAPO-18, which then promoted the adsorption and activation of NH_3 species. Over LaMn/Cu-SAPO-18 and SmMn/Cu-SAPO-18 catalysts, the reaction also follows both "L-H" and "E-R" mechanisms, and the "L-H" mechanism is the dominant one (Fig. 7) [28].

3. Effect of the preparation

The topological structure of silica-alumina type SSZ-39 and silica-alumina-phosphorus type SAPO-18 zeolite are double hexagonal rings connected by quadruple rings to form a cavity structure with eight rings. The AEI structure also comprises a pear-shaped cavity different from the CHA structure. The preparation process can exert a significant effect on its catalytic performance. Therefore, in the following sections, the effect of preparation method, effects of Si and Cu contents, and polymetallic-modified Cu-AEI zeolite will be discussed.

3.1. Preparation method

3.1.1. Synthesis of pure SSZ-39 and SAPO-18

The cage skeleton of SSZ-39 zeolite is composed of SiO_4 and AlO_4 tetrahedrons bonded by shared oxygen atoms. The synthesis of zeolite can be divided into traditional synthesis routes and new synthesis routes, including hydrothermal method, transcrystallization method and solvent-free method. The hydrothermal synthesis method involves

the introduction of a silicon and aluminum source into the reaction system using the coulomb forces between the template cation and the skeletal aluminum. They aggregate around the template agent to form crystal nucleus, which further grow into zeolite crystal by absorbing the surrounding inorganic material. The preferred method for the synthesis of SSZ-39 requires the use of simple alkyl-substituted cyclic quaternary ammonium cations as the organic structure directing agents (OSDAs) under alkaline conditions [29,30]. Moliner et al.[29] first synthesized Cu-SSZ-39 zeolite using N, N-dimethyl-3,5-dimethylpiperidine hydroxide as an organic structure directing agent. As shown in Fig. 8, this catalyst exhibited noticeably higher activity than Cu-SSZ-13 catalyst in a wide temperature range for the NH_3-SCR reaction. Cu-SSZ-39 maintains the high SCR activity even after hydrothermal treatment at 600 or 750 °C. In recent years, N,N -dimethyl-3,5-dimethylpiperidine and N,N -dimethyl-2,6-dimethylpiperidine quaternary ammonium molecules have been most extensively studied. Dusselier et al.[31] and Ransom et al.[32] illustrated that the promotion of the zeolite crystallization process by different template agents follow the order of trans-N, N-dimethyl- 3,5 -dimethylpiperidine > cis-N, N-dimethyl- 3,5 -dimethylpiperidine > N, N-diethyl-cis- 2,6 -dimethylpiperidine cation. As the amount of trans-isomer of the template agent will affect the aluminum content in the zeolite skeleton. In addition, the cis/trans ratio of OSDA used in the synthesis process also affects the NH_3-SCR activity. Nevertheless, the high price and the difficulty in the synthesis of the structure directing agents limited the large-scale production and application of SSZ-39.

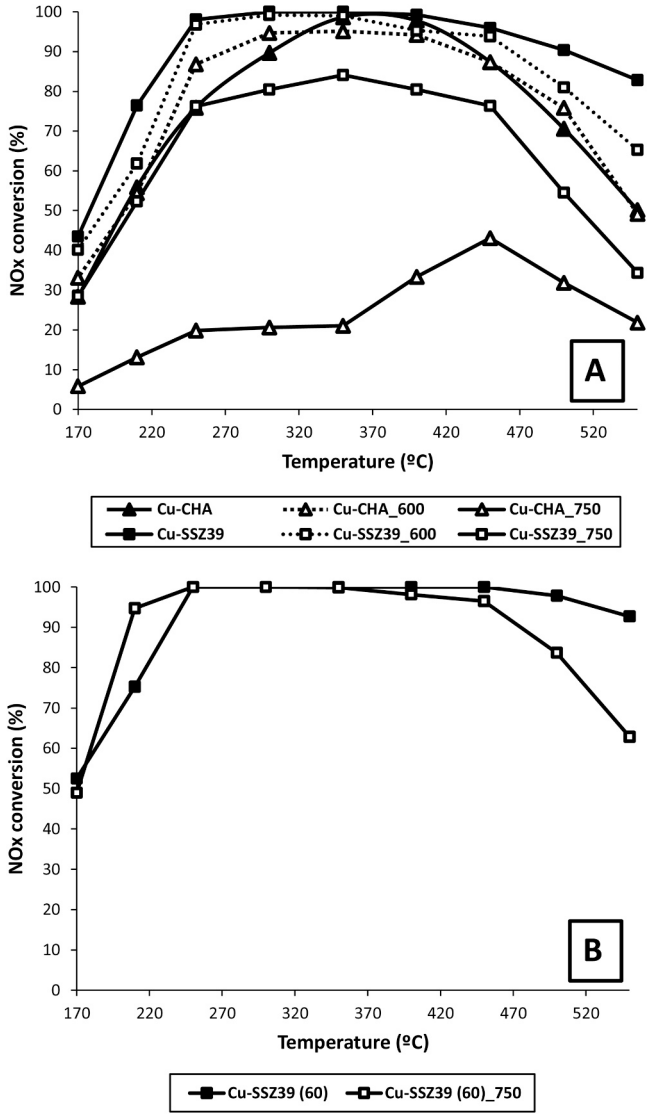

Fig. 8. NH_3-SCR of NO_x activity using severe reaction conditions in the presence of water and high space velocity for (A) Cu-SSZ-39 and Cu-CHA without hydrothermal steaming treatment and after hydrothermal steaming at 600 or 750 ℃; and for (B)Cu-SSZ-39(60) partially exchanged (60%) without hydrothermal steaming treatment and after hydrothermal steaming at 750 °C. Reprinted from [29] with permission of Royal Society of Chemistry.

The trans-crystallization method was considered to be one of the most important synthesis routes for zeolite, especially for SSZ-39 zeolite. In general, inter-zeolite transformations occur mainly during the transformation of zeolites from low to high framework density. Due to the structural similarity between FAU and AEI (i.e., the presence of a double 6-membered ring (d6r) building units is the key to the interconversion route between zeolites) [33,34], FAU was used as the feedstock for the synthesis of SSZ-39. Notably, during the synthesis process the Si source was not fully utilized, resulting in a much lower Si/Al ratio in the SSZ-39 product than the initial gel. In order to obtain high Si/Al ratio, high-silica FAU zeolite can be used [35]. Sano et al. [36] converted FAU into the high-silica P-modified SSZ-39 zeolite by transcrystallization using tetraethylphosphine hydroxide (TEPOH) as the structure directing agent. After the hydrothermal treatment at 900 °C for 1 h and 4 h, over 90% NO conversion was obtained over the P-modified Cu-AEI zeolite (P/Al ratio of 0.37) at 300 °C (Fig. 9). The excellent NH_3-SCR activity and hydrothermal stability of the P-modified Cu-SSZ-39 catalyst demonstrated that the SSZ-39 catalyst still has tremendous potential for the removal of NO_x.

SSZ-39 zeolites can be prepared by inter-zeolite transformation from high-silica FAU zeolites[37–39]. However, the preparation of FAU zeolite usually requires complicated post-treatment processes, making the synthesis of SSZ-39 zeolites be too costly and not environmental benign. Accordingly, it is highly desirable to find low-cost zeolites (such as ZSM-5 and Beta) to replace FAU zeolite for the synthesis of SSZ-39, the conversion process strongly challenges the law from low to high skeletal densities [40–45]. Recently, Xiao et al. [46] have theoretically calculated that the stability energy between the OSDAs and zeolite framework (MFI, FAU, and BEA) is higher than that between the OSDAs and AEI zeolite framework (Fig. 10), which indicates that ZSM-5(MFI) and Beta(BEA) zeolites can be converted to SSZ-39 zeolite. As expected, they successfully synthesized SSZ-39 zeolite with ZSM-5 and Beta zeolites as the silica source by the interzeolite conversion, and SSZ-39 showed superior catalytic performance in the NH_3-SCR reaction. In contrast to the crystallization mechanism of SSZ-39 zeolite synthesized from FAU zeolite, a large number of easily decomposed single

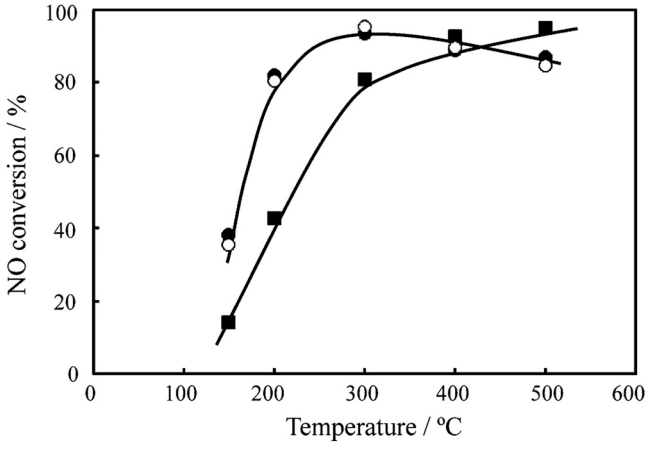

Fig. 9. NO conversions over the Cu-loaded AEI zeolite with a P/Al ratio of 0.37. (■) Fresh, (●) after hydrothermal treatment at 900 ℃ for 1 h, and (○) after hydrothermal treatment at 900 ℃ for 4 h. Reprinted from [36] with permission of Royal Society of Chemistry.

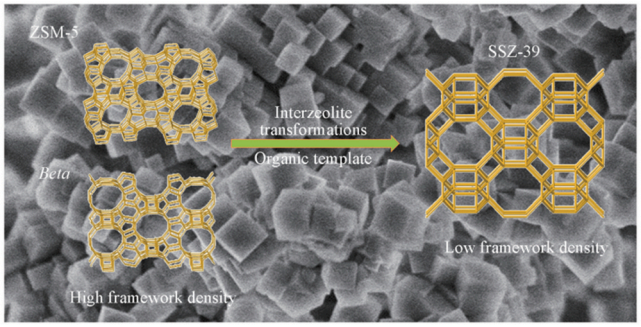

Fig. 10. Transformation synthesis of aluminosilicate SSZ-39 zeolite from ZSM-5 and Beta zeolite. Reprinted from [46] with permission of Royal Society of Chemistry.

five-membered rings (s5r) in the structure of MFI and Beta zeolites were broken into single four-membered (s4r) and single six-membered rings (s6r) under the hydrothermal transformation conditions, which were subsequently reconnected into d6r and further assembled to form SSZ-39 zeolite (Fig. 11)[47]. Nonetheless, due to the use of a large amount of water as a solvent under the hydrothermal conditions, the synthesis efficiency still needs to be improved.

In 2021, Xu et al.[48] first reported a solvent-free synthesis of SSZ-39 zeolite without adding water in the presence of N, N-dimethyl-3, 5-dimethylpiperidine (DMDMP) as an OSDA. As shown in Fig. 12, the prepared SSZ-39 displayed uniform sheet-like morphology with a thickness of about 200 nm, which was basically consistent with the SSZ-39 prepared by conventional hydrothermal synthesis method. Moreover, a higher SiO_2 utilization efficiency was achieved in the solvent-free synthesis method than the hydrothermal synthesis method. As a result, the yield of SSZ-39 zeolite (85%) is also higher than that prepared by the conventional method (65%). The synthesized Cu-SSZ-39 by Xu et al. presented a promising catalytic performance in the NH_3-SCR reaction before and after the hydrothermal treatment at 750 °C. Overall, the solvent-free method for synthesizing zeolite not only leads to excellent catalytic performance, space utilization, and high yield, but also effectively avoiding some chemical contamination, which provides an excellent opportunity for the future wide application of SSZ-39 zeolite.

Instead of using FAU zeolite as the raw material, Xu et al.[49] have successfully synthesized SSZ-39 by using conventional silica/aluminate sources for the first time. The catalyst possesses SiO_2/Al_2O_3 ratio of 12.8–16.8, and showed high activity for the NH_3-SCR reaction. The key to this success is to improve the Si/Al ratio in the raw materials for avoidance of MOR impure crystal formation. However, Si/Al in the product is still limited. Sano et al. [36] have fabricated SSZ-39 with Si/Al ratios of 13–20. Different from the synthesis of SSZ-13, there is still a limit on the Si/Al ratio for the synthesis of SSZ-39 zeolite. Therefore, SSZ-39 with higher Si/Al ratio is a future challenge and further investigation is needed.

Some consensus exists on the formation mechanism of SAPO zeolite, whereby silicon atoms enter the $AlPO_4$ skeleton by replacing a single skeletal phosphorus atom or a pair of phosphorus atoms. The introduction of Si disrupts the charge balance of the zeolite $AlPO_4$ skeleton (the skeleton is negatively charged), providing it exchangeable cations and sufficient strong acid centers on the surface. Therefore, it is widely used as the catalyst support. In 1994, Chen et al.[50] first synthesized SAPO-18 zeolite with different Si contents using N, N-diisopropylethylamine (DIPEA) as a structure directing agent, and revealed that the silicon atoms entered the zeolite skeleton by mono-substitution at low Si content and coupled substitution in the case of high Si content[51]. Later research showed that SAPO-18 is active for the NH_3-SCR reaction.

3.1.2. *Introducing of Cu into AEI zeolite*

Cu-AEI catalysts are usually prepared by aqueous solution ion exchange, solid-state ion-exchange and one-pot methods. The aqueous solution ion exchange method usually requires wet ion exchange with ammonium nitrate and copper salt solutions. For this method the content and type of Cu in the zeolite can be easily controlled by changing the concentration of the aqueous solution[21]. However, in the preparation large amounts of wastewater containing toxic and hazardous pollutants will be produced, which significantly limits the large-scale industrial production. To overcome this issue, solid-state ion exchange (SSIE) has gained interest as a new sustainable synthesis route, which is simple and the wastewater can be avoided to produce. Cu-SAPO-18 catalyst synthesized by the solid-state ion exchange method exhibited excellent SCR activity(Fig. 13) [52]. But the numerous ion exchange and calcination processes make the synthesis complicated.

In order to improve the efficiency of synthesis, one-pot method has been developed to obtain metal-containing zeolites by directly introducing active metal components during the crystallization process. This method has the following advantages: (1) the template agent can directly provide highly loaded and dispersed metal species, improving the metal utilization efficiency; (2) the metal loading and crystal size of zeolites can be effectively controlled; (3) the complexes are stable under alkaline synthesis conditions.

In 2014, Cu-SAPO-18 catalyst was synthesized directly by Corma's

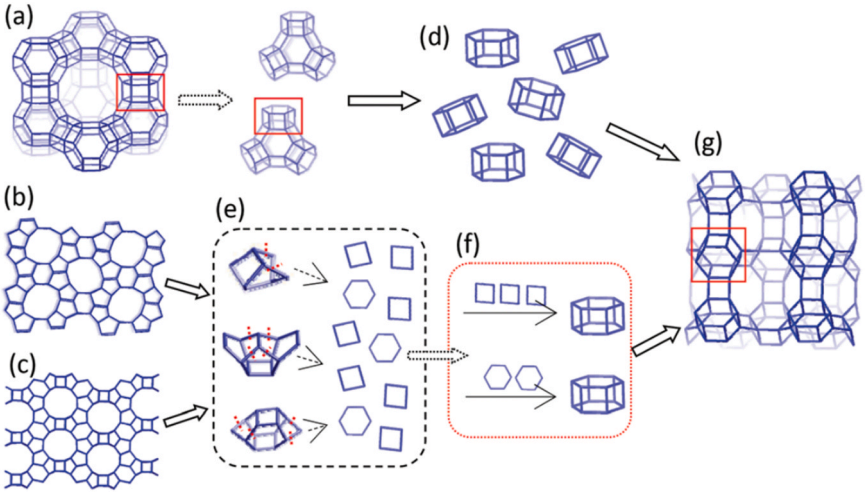

Fig. 11. Proposed synthesis mechanism of the inter-zeolite transformation of the AEI zeolite from FAU (a, d and g), MFI (b and e–g), and *BEA (c and e–g) zeolites. Reprinted from [47] with permission of Royal Society of Chemistry.

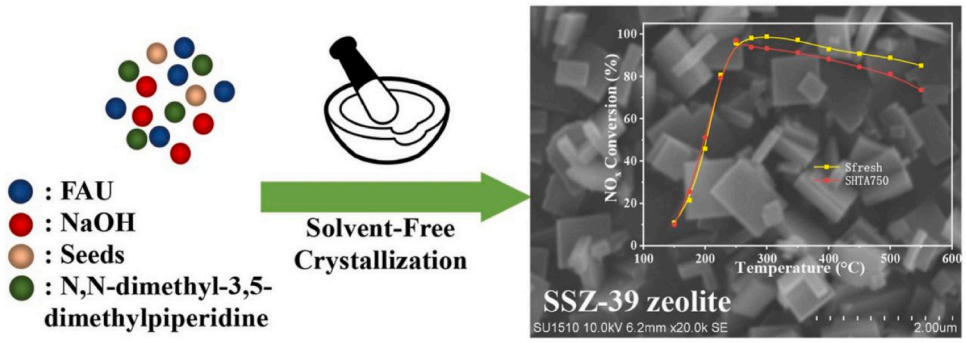

Fig. 12. SEM image of SSZ-39 zeolite synthesized by solvent-free route and NOx conversion versus temperature over the Cu-SSZ-39 catalysts before and after hydrothermal treatment (10% vapor in N_2 flow under 750 °C for 16 h) in NH_3-SCR with GHSV of 400000 h^{-1}. Reprinted from [48] with permission of Elsevier.

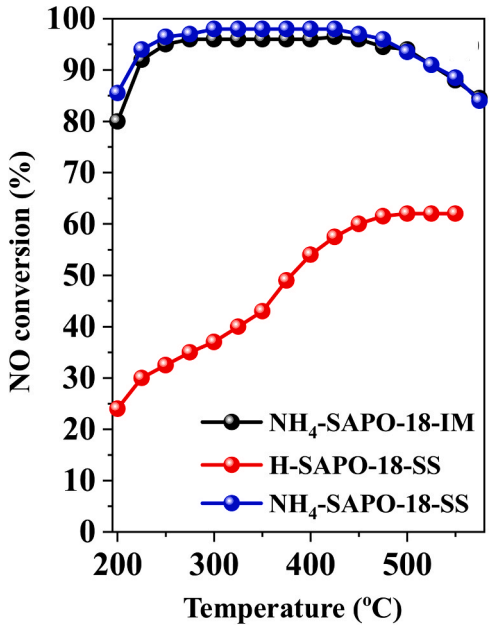

Fig. 13. NH_3-SCR activity for catalysts synthesized by SSIE and IM methods: (b) Cu-SAPO-18. Reprinted from [52] with permission of Elsevier.

group[53] using copper-amine complexes and N,N-dimethyl-3,5-dimethylpiperidine as dual structure directing agents. The catalyst prepared by the one-pot synthesis method exhibited superior SCR activity and hydrothermal stability compared to the sample prepared by the ion exchange method. As shown in Fig. 14, the NO_x conversion was maintained above 90% at 200–475 °C after hydrothermal aging treatment at 750 °C for 13 h. In the one-pot synthesis of Cu-SAPO-18, a large amount of deionized water needs to be added due to the high viscosity of the gel. Hence, the production of a large amount of waste solution during the synthesis process is an important issue limiting its large-scale production. Rani et al.[54] investigated the waste mother liquor, and found the presence of primary structural units with zeolite memory in the mother liquor, which can aggregate to form live nuclei when raw materials are added. On this basis, Guo et al. [55] proposed a green and efficient way to synthesize Cu-SAPO-18 by the one-pot method using different amount of mother liquor. Compared with conventional synthesis methods, the sample synthesized by this method exhibited better high-temperature SCR activity and hydrothermal stability. Moreover, this method reduces the costs as well as the waste solution, which are essential for the future large-scale industrial application of the one-pot method.

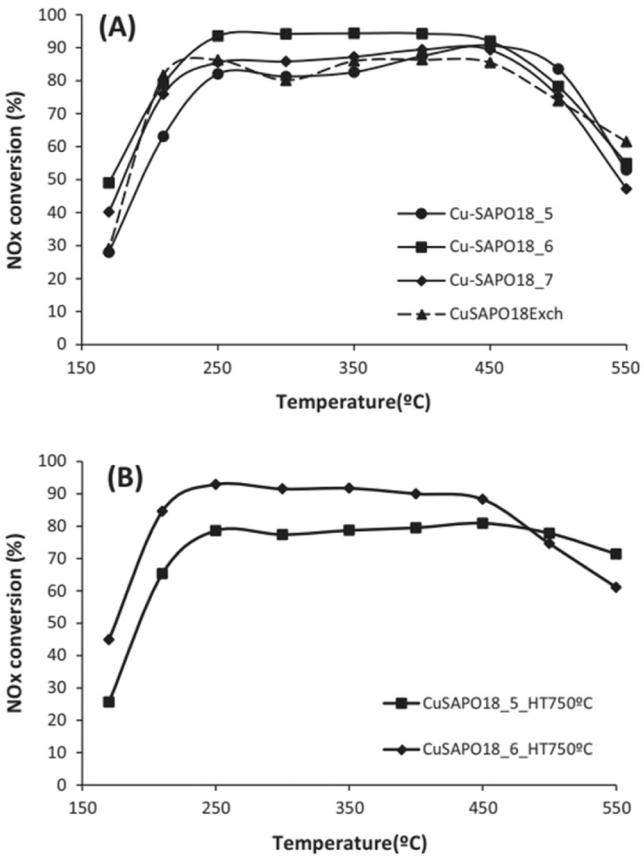

Fig. 14. Catalytic activity for the SCR of NO_x reaction of Cu-SAPO-18 materials synthesized at 175 °C using DMDMP after calcination at 550 °C and Cu-exchanged SAPO-18 (A) and after steam treatment at 750 °C for 13 h (B). Reprinted from [53] with permission of Elsevier.

3.2. *Effect of Si content*

The Si content is an essential parameter in the zeolite framework. Different Si doping into the neutral framework of AlPOS can lead to various Si coordination structures [Si(xOAl) (x = 0–4)], which further determine the nature of various acids in aluminosilicate zeolite, thus affecting the NH_3-SCR activity of Cu-based zeolite catalyst.

Most Cu-AEI catalysts used for the NH_3-SCR reaction have relatively high ratio of Si/Al (Si/Al>8) [29,36,56–58]. Ming et al. [59] found that the Si content can affect the amount of acid sites as well as the isolated Cu^{2+} species on Cu-SAPO-18 catalyst. Higher Si content would lead to

more acid sites and Cu^{2+} species in a specific range, both of which are favorable for the NH_3-SCR activity. However, in the case of high Si content the zeolite structure was more easily destroyed under the hydrothermal treatment due to a large amount of Si(0OAl) structure. Chen et al.[60] reported that the activity of Cu-SAPO-18 catalyst synthesized by the one-pot method also followed the above rule (Fig. 15). The ^{29}Si MAS NMR, NH_3-TPD and EPR results revealed that the Si content in the initial gel affects the coordination structure of the skeletal Si, which in turn affects the acidity and Cu distribution of Cu-SAPO-18 catalyst. The amount of acid sites and the isolated Cu^{2+} first increase and then decrease with increasing Si content. The more Si (xOAl) (x = 1–3) structures exist, the more strong acid sites are generated in the Cu-SAPO-18 catalyst. These strong acid sites favor the stabilization of isolated Cu^{2+} ions, thus enhancing the stability of isolated Cu^{2+} ions and zeolite framework in the hydrothermal treatment. These facts indicate that the SCR activity and stability of Cu-SAPO-18 catalyst are closely related to the Si content. Consequently, Cu-SAPO-18 catalyst with appropriate Si content is promising for the removal of NO_x from diesel exhaust.

Different Si coordination structures and acid sites exert different stabilizing abilities for Cu^{2+} ions in the hydrothermal treatment [61]. Shan et al.[62] compared the NH_3-SCR activities of the Al-rich Cu-SSZ-39(Si/Al<8) and Cu-SSZ-13 catalysts (Fig. 16). Cu-SSZ-39 maintained outstanding activity after hydrothermal treatment at 850 °C, while Cu-SSZ-13 was almost inactive after the same hydrothermal treatment. Compared with Cu-SSZ-13, Cu-SSZ-39 zeolite contains more paired skeletal Al with high stability, and a large amount of Cu^{2+}-2Z in Cu-SSZ-39 is coordinated with the paired skeletal Al, with fewer uncoordinated Al sites remained. Thus the active Cu^{2+} species are more stable. In addition, SSZ-39 has a more zigzag pore structure, which can effectively avoid the exit of isolated $Al(OH)_3$ from the pores of the AEI zeolite framework at high temperatures, making SSZ-39 zeolite maintain an intact structure after cooling.

3.3. Effect of Cu content

It is well known that the NH_3-SCR performance of Cu-based zeolite is closely related to the nature and distribution of Cu species, which is affected by the Cu content. For Cu-SAPO-18 catalyst, Gao et al.[63] demonstrated that the CuO content increased with increasing Cu/Al mass ratio, while the Cu^{2+} content isolated from the catalyst surface increased and then decreased. The sample with the highest Cu^{2+} content showed the best SCR activity. Among a series of Cu-SAPO-18 catalysts, $Cu_{4.42}$-SAPO-18 catalyst exhibited the highest SCR activity in a wider temperature range (200–450 °C), and over 80% NO conversion can be obtained at 200 °C, which attributed to the highest amount of Cu^{2+} species isolated from the $Cu_{4.42}$-SAPO-18 catalyst [26]. The effect of Cu content on the catalytic activity of Cu-SAPO-18 catalyst was also investigated by Ming et al.[59](Fig. 17). The amount of Cu^{2+} and CuO species increased with increasing Cu loading (1.53 wt% – 3.51 wt%). $Cu_{3.51}$-SAPO-18 catalyst showed the highest NO conversion at low temperatures (200–300 °C), but the conversion decreased significantly at high temperatures (400–575 °C). The increased CuO species promoted the oxidation of NH_3, resulting in the decrease of the high-temperature activity. Among them, $Cu_{2.49}$-SAPO-18 with 2.49 wt% Cu loading exhibited excellent NH_3-SCR activity and hydrothermal stability, which can be attributed to the appropriate Cu^{2+} content and the relatively small number of CuO species. It is believed that appropriate amount of Cu would facilitate the NH_3-SCR reaction [64–67].

Recently, Fu et al.[21] found new Cu-active species by EPR

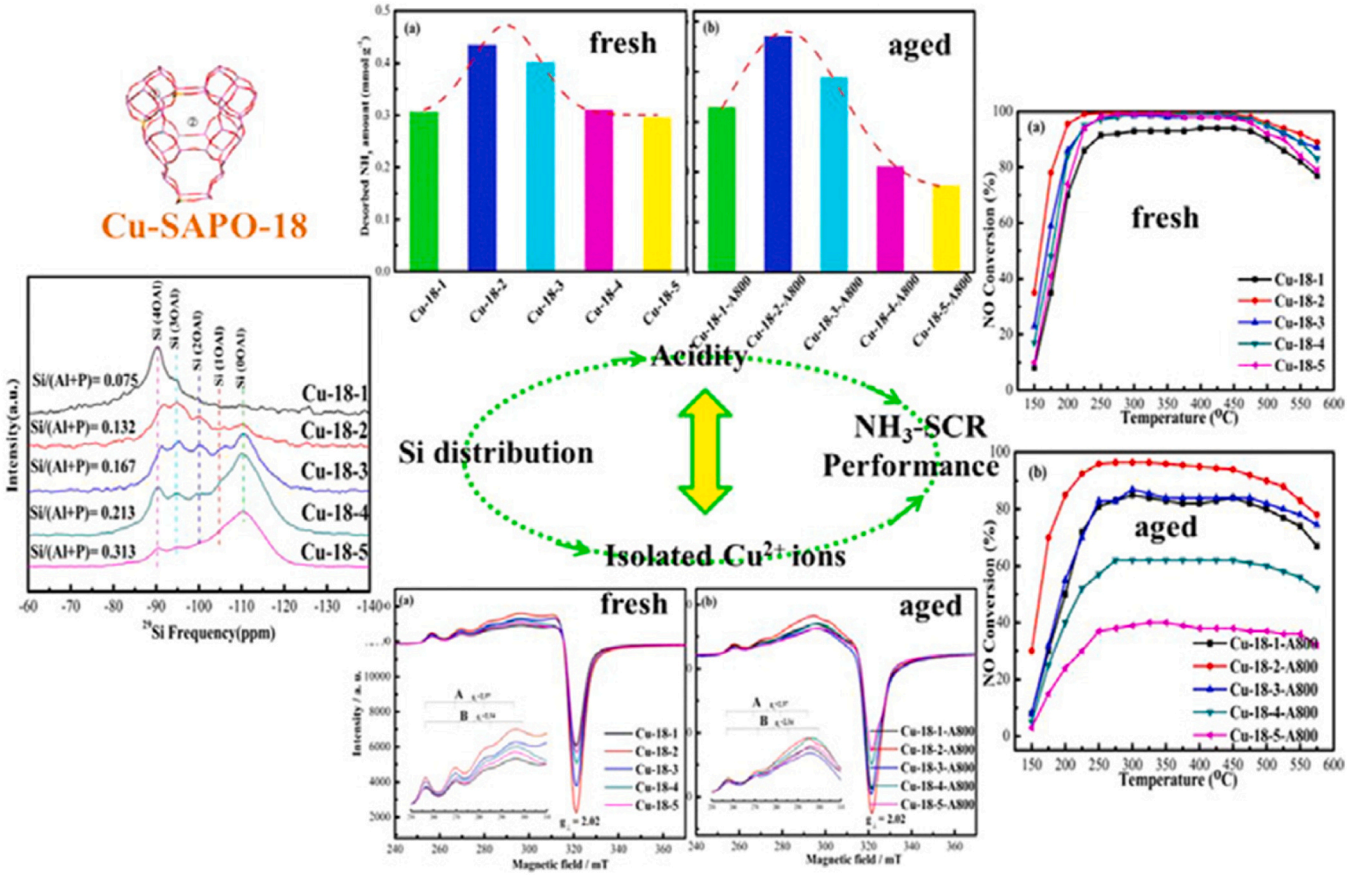

Fig. 15. The NH_3-SCR activity, acid amount, various Si coordination structures, the location and the amount of isolated Cu^{2+} ions over fresh and hydrothermal aged Cu-SAPO-18 samples obtained from NH_3-TPD, 29Si MAS NMR and EPR. Reprinted from [60] with permission of Elsevier.

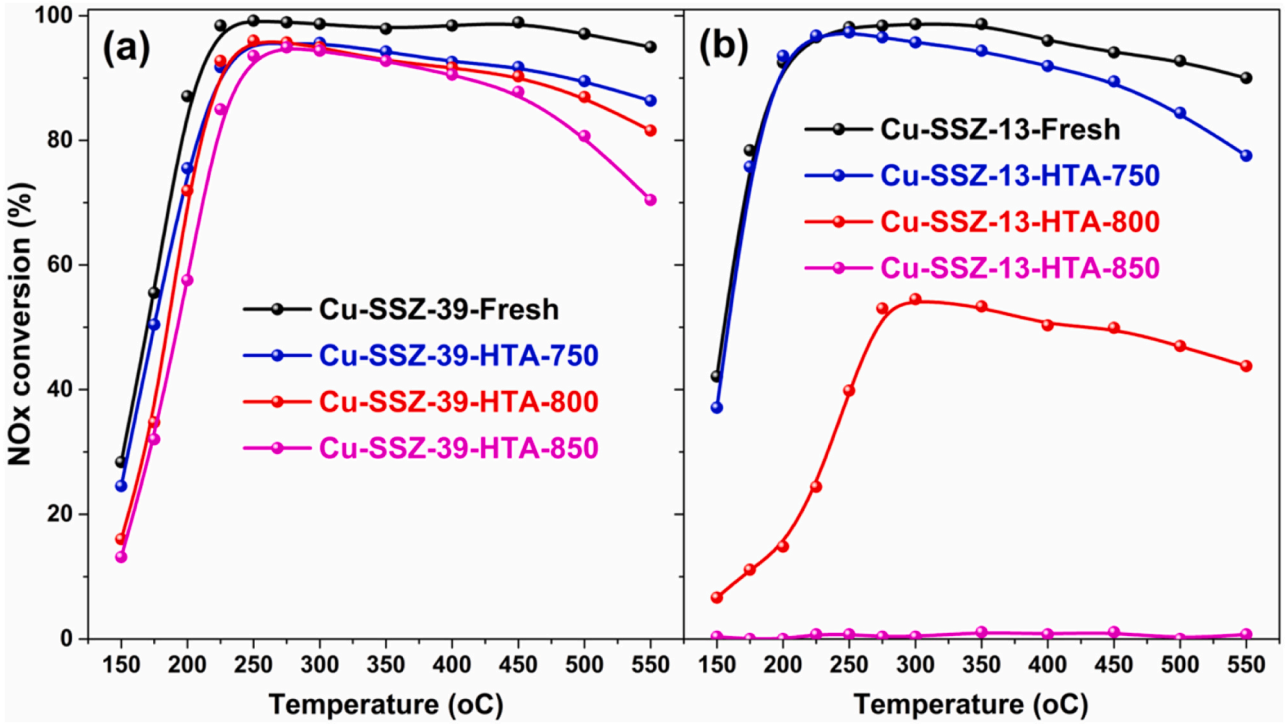

Fig. 16. NO_x conversion as a function of temperature in NH_3-SCR reaction over fresh, 750, 800, and 850 ℃ hydrothermally aged (a) Cu-SSZ-39 and (b) Cu-SSZ-13 catalysts. Conditions: 500 ppm NO, 500 ppm NH_3, 5 vol% H_2O, and 5 vol% O_2 balanced with N_2, GHSV = 250, 000 h^{-1}. Reprinted from [62] with permission of Elsevier.

technique. They demonstrated both $[Cu(OH)]^+$ and Cu^{2+} species isolated from Cu-SSZ-39 zeolite were present at low Cu exchange levels, and both species increased with increasing Cu content. When Cu content reached 2.9 wt%, the amount of CuO_x increased substantially due to the aggregation of Cu ions, which led to an increase of NO_x conversion at low temperatures (<300 ℃) and a decrease of NO_x conversion at high temperatures (>450 ℃) over Cu-SSZ-39 catalyst.

The content of Cu can affect the amount of isolated Cu ions ($[Cu(OH)]^+$ and Cu^{2+}) and the number of sites that can accommodate isolated Cu ions after the hydrothermal treatment (Al detachment from the zeolite framework is accompanied by the formation of irreversible $CuAl_2O_4$ species). Therefore, Cu-AEI zeolites possessed the higher hydrothermal stability than Cu-CHA zeolites. For Cu-based zeolite catalysts, the location of the active site is dependent on the structure of the zeolite. For Cu-ZSM-5 catalyst, the dimeric Cu is preferentially distributed in 6 R, while the isolated Cu^{2+} ions are distributed in 5 R [68]. In the case of Cu-Y catalyst, the active Cu^{2+} ions are preferentially located on the surface of the D6R subunit in the FAU structure near the sodium salt pores [69,70]. For Cu-CHA catalyst, Fickel et al.[8] suggested that Cu^{2+} are all located within the D6R windows of Cu-SSZ-13, while Kwak et al.[7] proposed two different Cu active sites are located in the 6R of the Cu-SSZ-13 and within the cage, respectively.

In the case of Cu-SAPO-18 catalyst, Li et al.[26] proposed that isolated Cu^{2+} ions were located in the pear-shaped cavity and preferred the vicinity of the 6R face of Cu-SAPO-18. For the Cu-SSZ-39 catalyst, isolated Cu^{2+} ions are located on one 6-ring face with two tetrahedral Al of D6R unit [21]. Accordingly, to achieve the best activity of Cu-SSZ-39 catalyst, the degree of Cu ion exchange should reach the level of the D6R site as much as possible, but there should be no Cu remaining. Assuming that $[Cu(OH)]^+$ ions also occupy the outer skeleton sites, they will fully aggregate into CuO_x after the hydrothermal treatment because they are not very stable under the hydrothermal conditions, which is detrimental to the SCR activity of the catalyst.

3.4. Promoter modified Cu-AEI zeolite

In addition to modifying the content of Si and the Cu active site of Cu-AEI, introducing other metals is also an effective way to improve the SCR performance. The synergistic interaction between Cu and heteroatoms can lead to increased active sites, enhanced acid sites and redox properties, thus improving the performance of zeolite catalyst [71,72].

Gao et al.[73] introduced lanthanides (La, Ce, Nd, Gd, Tb, Ho or Lu) into the Cu-SAPO-18 catalyst by ion exchange method. CeCu-SAPO-18 and TbCu-SAPO-18 catalysts exhibited higher activity than Cu-SAPO-18 catalyst in the whole investigated temperature range, which may be due to the added promoter affecting the interaction between Cu ions and SAPO-18. Ce doping promoted the migration of Cu^{2+} ions to the position (within the 8MRs cage) favoring the catalytic activity. In comparison, other lanthanide ions exerted little or negative effect on the migration of Cu^{2+} ions. For CeCu-SAPO-18 catalysts with different Ce contents (0–3.15 wt%) prepared by one-pot method, the addition of a small amount of Ce (0.13–0.31 wt%) not only broadened the activity temperature window but also greatly improved its hydrothermal stability. As the Ce loading reached 3.15 wt%, it was introduced into the ion-exchange site of Cu-SAPO-18 zeolite in the form of Ce^{3+}, which can affect the distribution of silica-aluminum atom coordinated in the AEI framework (producing more framework aluminum). As a result, the amount of Brønsted acid sites and Cu^{2+} are increased, which led to enhanced low-temperature activity (<200 °C) of the CeCu-SAPO-18 catalyst. Ming et al.[28] investigated the effect of multi-metal doping on the SCR activity of zeolite. They first synthesized Mn/Cu-SAPO-18 catalyst with high NH_3-SCR activity and hydrothermal stability by adjusting the concentration of the mixed solution of Mn^{2+} and NH_4^+. Then they introduced La^{3+}, Ce^{3+}, Sm^{3+} or Zr^{4+} metal ions to Mn/Cu-SAPO-18, respectively. It was found that the doping Sm resulted in improved NH_3-SCR activity and hydrothermal stability to the greatest extent, and more Cu^{2+} and acid sites were responsible for the highest catalytic performance.

The catalytic performance of Cu-SSZ-39 catalyst can also be

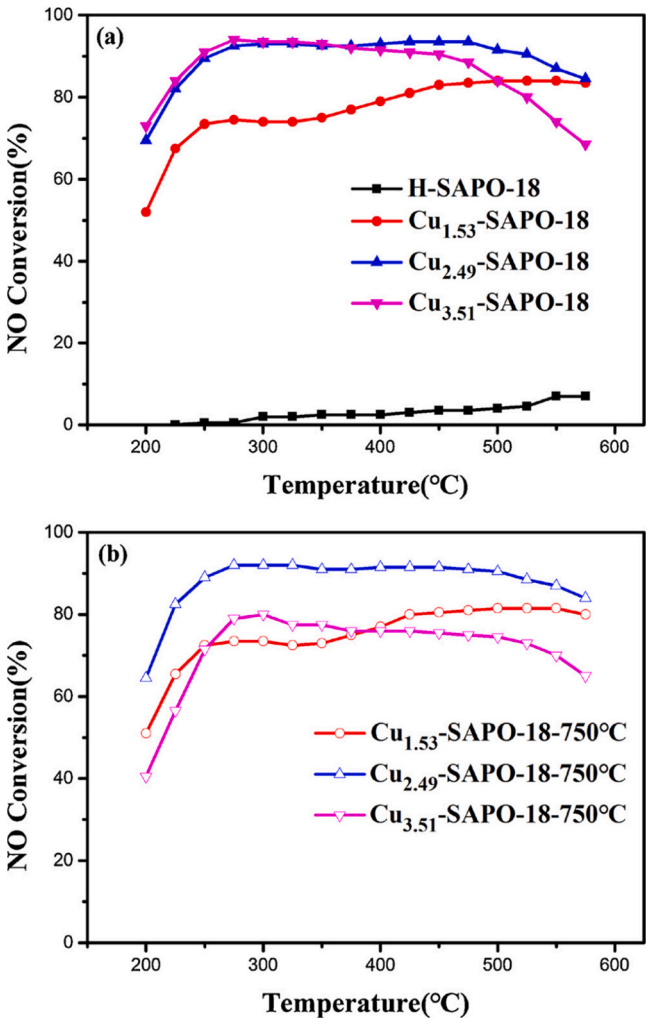

Fig. 17. NH_3-SCR performance of the fresh and aged Cuy-SAPO-18 catalysts. Reprinted from [59] with permission of Elsevier.

improved by the addition of other metals. The introduction of Ce or Mn improved the redox property and the amount of surface acid sites of Cu-SSZ-39 catalyst, which enhanced the SCR activity and hydrothermal stability [25]. Since the hydrothermal stability is one of the key characteristics of Cu-AEI, in the following section it will be discussed in more detail.

4. Hydrothermal stability

For diesel vehicle after-treatment system, the regeneration of the DPF next to the SCR unit would create high-temperature surroundings (above 650 °C). Therefore, the SCR catalyst should possess excellent hydrothermal stability to make the catalyst work stably within the expected lifetime. In general, the hydrothermal aging of zeolite leads to the dealumination process, which is caused by the attraction of H_2O molecules to aluminum sites when H_2O is present at high temperatures, thus resulting in the separation of aluminum atoms from their respective sites [8,74], the sintering of alumina and mixed oxides outside the frame, the structure change of the zeolite framework, or even the collapse of the zeolite skeleton with significant loss of acid sites [75–78]. For Cu ion exchanged zeolites, the framework structures of medium-pore and large-pore zeolites (e.g., Cu-MFI, Cu-BEA) are more susceptible to be changed after the hydrothermal treatment than those of small pore zeolites (e.g., Cu-CHA, Cu-AEI) [79,80]. The reason is that the pore size of small pore zeolites such as CHA and AEI (kinetic diameter of 3.8 Å) limits the $Al(OH)_3$ (kinetic diameter of about 5.03 Å). This prevents the formation of bulk alumina outside the skeleton and allows the reorganization of monomeric aluminum species within the framework vacancies in the course of decreasing the temperatures, thus maintaining the integrity of the zeolite skeleton.

CHA and AEI small-pore zeolite catalysts also exhibit different hydrothermal stability due to the differences in their pore structures. After the hydrothermal treatment at 850 °C for 16 h, Cu-SSZ-39 maintained its excellent NH_3-SCR activity, whereas the Cu-SSZ-13 catalyst lost its activity completely [61]. The main reason is that SSZ-39 zeolite contains more paired framework Al, which leads to more hydrothermally stable Cu^{2+}-2Z species, and allows Cu-SSZ-39 to accumulate less CuO_x during the hydrothermal aging process. XRD results can further demonstrate that the hydrothermal process causes the Cu-SSZ-13 zeolite framework to collapse while the Cu-SSZ-39 catalyst maintains structural integrity (Fig. 18). The superior hydrothermal stability of Cu-AEI zeolite relative to Cu-CHA zeolite was also reported by Lin et al.[24]. As shown in Fig. 19, 1 wt% Y modified catalyst (Cu/Y1.0-SSZ-39) displayed high NH_3-SCR activity even after the hydrothermal aging at 900 °C for 10 h. The NO_x conversion was higher than 70% at 200–550 °C and up to 94% at 300 °C. In contrast, Cu/Y-CHA catalysts almost lost their NH_3-SCR activities after the same hydrothermal treatment. The significant difference in hydrothermal stability exhibited by Cu-AEI and Cu-CHA catalysts may be due to the complex pores of SSZ-39, which provide a more stable structure, and the longer pore spacing of SSZ-39 zeolite can better hinder the diffusion of H_2O molecules and the migration of Al atoms. It is necessary to further investigate the factors affecting the hydrothermal stability of Cu-AEI, which could provide some insights for further improving the hydrothermal stability.

The hydrothermal stability of Cu-based zeolite catalyst is dependent on the stabilities of the skeletal Al atoms and the Cu active species [61, 81–83]. On one hand, preventing the isolated Cu ions (including $[Cu(OH)]^+$ and Cu^{2+}) active sites from aggregating into bulk CuO_x species is the key to maintain the activity of Cu-AEI catalyst. On the other hand, the number and position of the framework Al atoms determine the maximum content of ionic sites outside the framework. This means that the hydrothermal process of zeolite framework dealumination will reduce the adsorption sites of Cu ions. When Al detaches from the framework, it will irreversibly form inactive $CuAl_2O_4$ species[84,85]. Fu et al.[21] found a significant correlation between the hydrothermal stability of Cu-SSZ-39 and the Cu content. Cu-SSZ-39 with higher Cu content (especially the zeolite with more isolated Cu^{2+} ions) exhibited better SCR activity, which may be due to the mutual protection between the isolated Cu^{2+} ions and the framework Al atoms. Moreover, Cu^{2+} ions protect the Al atoms from H_2O erosion during the hydrothermal treatment. Wang et al.[25] introduced Mn to Cu-SSZ-39 by ion-exchange, and found the synergistic interaction between Mn and Cu-SSZ-39 led to increased active species, while inhibiting the formation of large CuO_x on the external framework. Therefore, an increased activity can be obtained even after the hydrothermal aging treatment at 850 °C.

Ming et al.[28] optimized MnCu-SAPO-18 with the addition of La^{3+}, Ce^{3+}, Sm^{3+} or Zr^{4+} ions, respectively, and found the co-doping of Sm maximized the hydrothermal stability. Other studies showed that yttrium (Y) is superior to other rare earth elements (Ce, La, Sm and Yb) in improving the hydrothermal stability of Cu-based zeolite catalysts [86–88]. Lin et al.[24] introduced Y^{3+} into Cu-SSZ-39 zeolite and the high activity can be maintained after the hydrothermal treatment at 900 °C for 10 h (Fig. 20). The electron repulsion of Y^{3+} induced ZCuOH into the ion-exchange sites of the internal channels of Cu/Y-SSZ-39 zeolite, further enhancing the hydrothermal stability of ZCuOH through the spatial site blocking effect of surface Y^{3+} and Z2Cu on H_2O molecules. As shown in Fig. 9, the activity of P-modified SSZ-39 zeolite was even enhanced after the hydrothermal treatment[36]. It may be due to the fact that the hydrothermal process causes Cu ions to migrate to the effective active site for the NH_3-SCR reaction. These studies provide guidelines for the rational design of Cu-based zeolite catalyst that can be

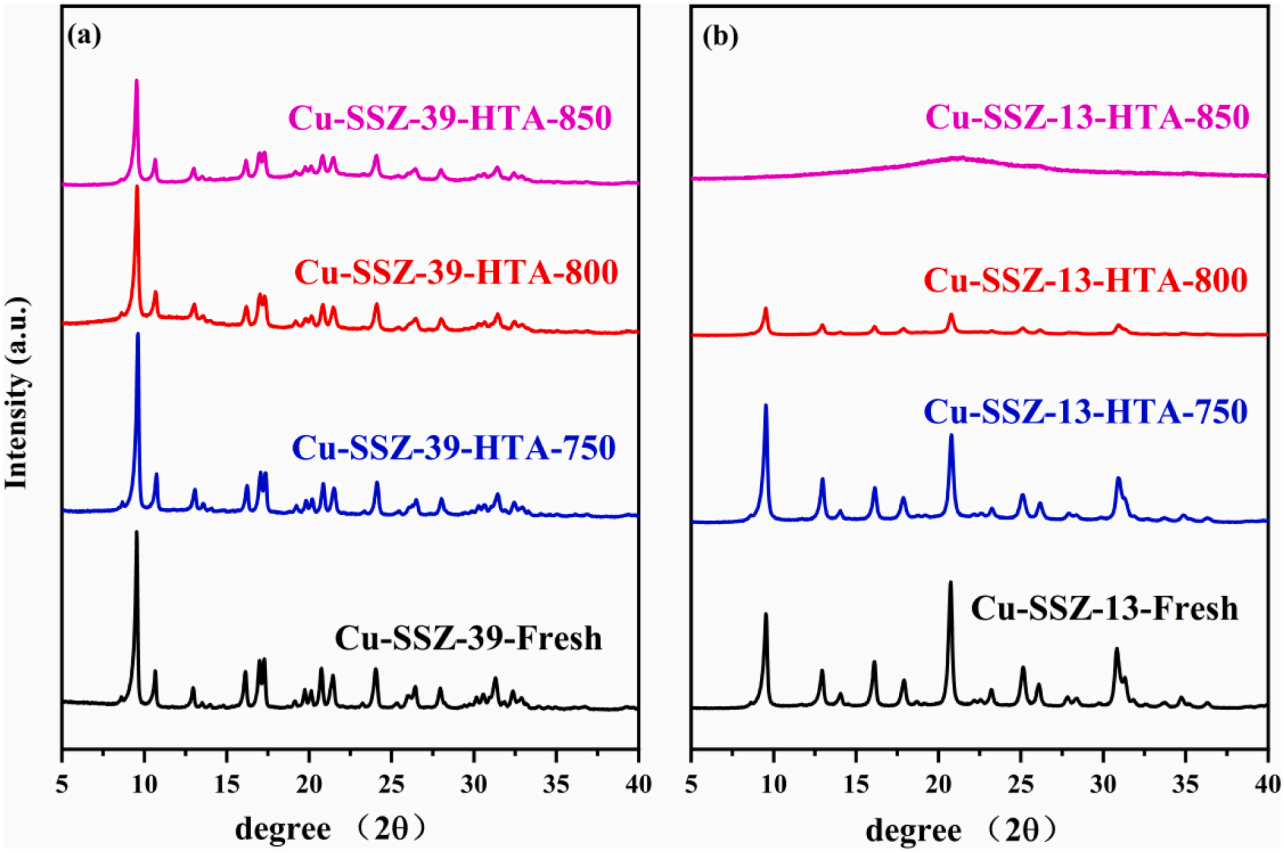

Fig. 18. XRD patterns of (a) Cu-SSZ-39 and (b) Cu-SSZ-13 before and after hydrothermal aging at 750, 800, and 850°C. Reprinted from [62] with permission of Elsevier.

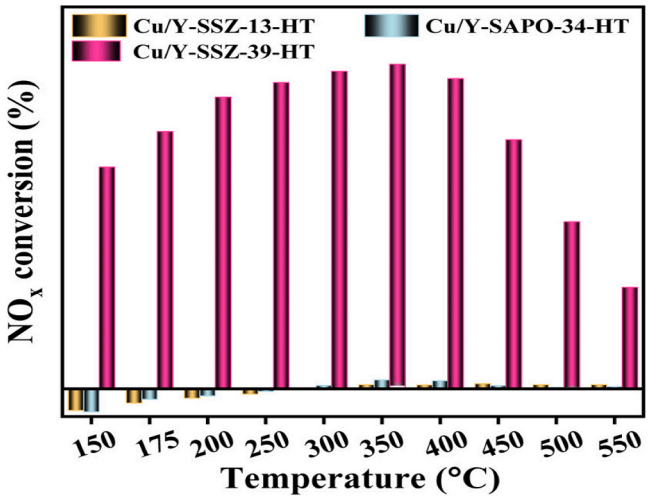

Fig. 19. NH_3-SCR activity of Cu/Y-CHA-HT and Cu/Y-SSZ-39-HT. Reprinted from [24] with permission of American Chemical Society.

adapted to NH_3-SCR reaction under severe conditions.

5. Low-temperature NH_3-SCR activity

In order to improve the low-temperature NH_3-SCR activity, the fabrication of bimetallic AEI zeolite is an effective method. Sun et al. [89] compared the activities of Cu/Fe-SSZ-39, Fe-SSZ-39 and Cu-SSZ-39 catalysts for the NH_3-SCR of NO_x. As shown in Fig. 21, the low-temperature activity of Fe-SSZ-39 is much lower than that of Cu-SSZ-39 catalyst. Martin et al.[58] also reported that Fe-SSZ-39 catalyst is not active, with only about 30% NO conversion obtained at 250 ℃. Compared with Cu-SSZ-39 and Fe-SSZ-39, Cu/Fe-SSZ-39 catalyst exhibited higher low-temperature activity. About 90% NO conversion was achieved over Cu0.42/Fe0.16-SSZ-39 catalyst, in which Cu/Al and Fe/Al molar ratios are 0.42 and 0.16, respectively. Characterization identified that isolated Cu^{2+} and Fe^{3+} ions are the active centers [90, 91]. Fe^{3+} is primarily located at 6MR sites, while Cu^{2+} active centers preferentially occupy more active 8MR sites. More isolated Cu^{2+} and Fe^{3+} active centers in Cu/Fe-SSZ-39 catalyst promoted its low-temperature reactivity [89].

Regarding SAPO-18 catalyst, the addition of Ce can lead to enhanced low-temperature NH_3-SCR activity and the optimum loading of Ce is 0.31 wt%. The NH_3-SCR reaction rate at 150 ℃ over CuCe-SAPO-0.31 catalyst is about 1.7-fold of that over Cu-SAPO-18 catalyst (Fig. 22) [27]. The introduction of Ce was found to affect the distribution of silicon and aluminum atoms coordinated in the AEI-type skeleton, leading to more active Cu^{2+} species and increased acidity of CuCe-SAPO-18 catalyst [27]. All of these contribute to enhancing the low-temperature NH_3-SCR activity. As a large amount of NO_x is emitted during the cold start stage, low-temperature activity should be a challenge for the Cu-AEI catalyst.

6. Catalyst deactivation

6.1. *Sulfur poisoning*

It is well known that Cu-based zeolite catalysts are sensitive to SO_2 [92–94]. Since a certain amount of sulfur is present in diesel inevitably, after combustion SO_2 will emit and accumulate on the catalyst surface, thus inhibiting the NH_3-SCR reaction [95]. The mechanism of SO_2

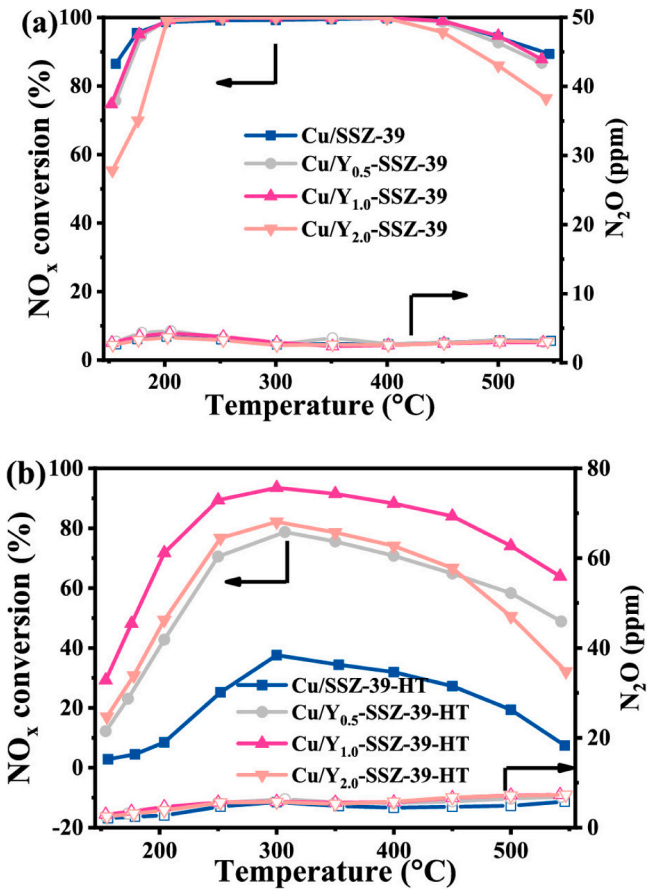

Fig. 20. NH_3-SCR performance of (a) fresh and (b) HTA catalysts after 900 °C for 10 h. Condition: 220 ppm NH_3, 200 ppm NOx, 10 vol% O_2 and 5 vol% H_2O balanced with N_2, and the total space velocity of 40 000 h^{-1}. Reprinted from [24] with permission of American Chemical Society.

poisoning on Cu-based catalysts includes two types: one is the accumulation of $(NH_4)_2SO_4$ covering the active sites and blocking the zeolite pore channels, preventing the reaction from proceeding, and the other attributes to the poisoning of the active metal by SO_2. For instance, after SO_2 oxidation to SO_3, it combines with Cu to form $CuSO_4$, which limits the redox cycle of Cu^{2+}/Cu^{+} and inhibits the adsorption and activation of the reactants on the active sites [96,97]. In the co-presence of H_2O and SO_2, the sulfide can be converted to H_2SO_4, thus promoting the generation of $CuSO_4$ and causing more severe deactivation of Cu zeolites. Fortunately, the poisoned catalysts can be recovered in most cases by the high-temperature treatment [96,98–101], and the recovering degree depends on the type of sulfate generated.

The degree of sulfur poisoning on the catalyst can be influenced by factors such as reaction temperature[101], gas composition[102] and sulfur content[103]. Du et al.[104] investigated the effect of sulfur poisoning on the performance of the Cu-SSZ-39 catalyst for NH_3-SCR(see Fig. 23). Cu-SSZ-39 catalysts were sulfated at 200 °C, 400 °C and 600 °C for 10 h in the presence of 10% H_2O and 50 ppm SO_2. The NO_x conversion over the sulfated Cu-SSZ-39 catalyst was decreased in the low temperature range (<275 °C), especially for the samples after sulfation at 200 °C or 400 °C. For these two catalysts, the accumulation of H_2SO_4 is the main reason for the decrease of the low-temperature activity. In the case of 600 °C sulfation treatment, the SCR activity decrease is mainly due to the formation of $CuSO_4$ species on the $Cu(II)(OH)^{+}$ site. This indicates that the different sulfation temperature led to different poisoning effect and poisoning mechanism. After regeneration at 600 °C for 2 h, the SCR activities of all sulfated Cu-SSZ-39 catalysts were partially recovered and significantly lower than that of fresh Cu-SSZ-39. This suggests that the sulfation led to the irreversible deactivation [98].

Besides the sulfated temperature, sulfur content is also closely related to the poisoning effect. Fig. 24 shows the SCR activity of the Cu-SAPO-18 catalyst before and after sulfation at different sulfur contents (50 ppm,100 ppm and 200 ppm)[95]. Compared with the fresh catalyst, the NO_x conversion over the sulfated Cu-SAPO-18 catalyst in the low temperature range was decreased, and the decrease was more pronounced with increasing SO_2 concentration. The poisoning is due to the formation of sulfite and sulfate covering the Cu^{2+} active site, especially the isolated Cu^{2+} sites in the pear-shaped cavity of the AEI structure are more severely poisoned by SO_2 than the Cu^{2+} sites on the double 6-membered ring (D6R). Furthermore, in the presence of NH_3, sulfate on the sulfated catalyst can react with NH_3 to form $(NH_4)_2SO_4$ [100,105], which could also cover the Cu^{2+} active site and further inhibit the low-temperature activity. With SO_2 concentration increasing from 50 to 200 ppm, the content of sulfur-containing species on the catalyst surface is increased. As the temperature is above 350 °C, the sulfated sample underwent a similar NO conversion to the fresh catalyst, which is ascribed to the decomposition of $(NH_4)_2SO_4$ at high temperatures[100]. It is noted that after the sulfation the high-temperature activity is seldom

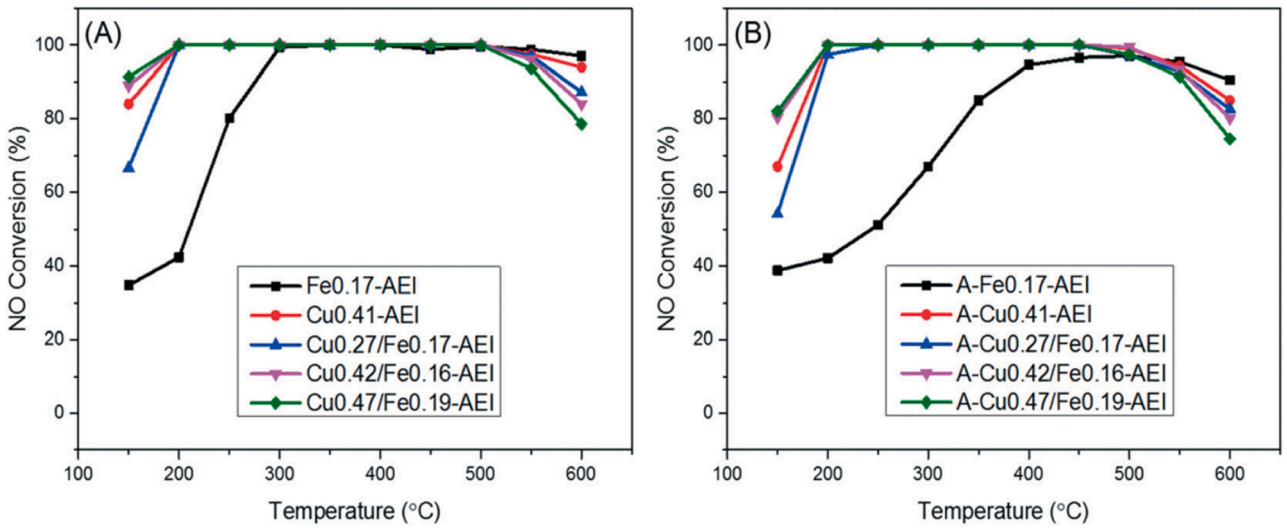

Fig. 21. SCR performances of Cu/Fe-AEI catalysts with various Cu concentrations: (A) fresh and (B) hydrothermally aged. Reaction conditions: 500 ppm NO, 500 ppm NH_3, 10% O_2, 5% H_2O, and N_2 balance; GHSV: 80 000 h^{-1}. Reprinted from [89] with permission of Royal Society of Chemistry.

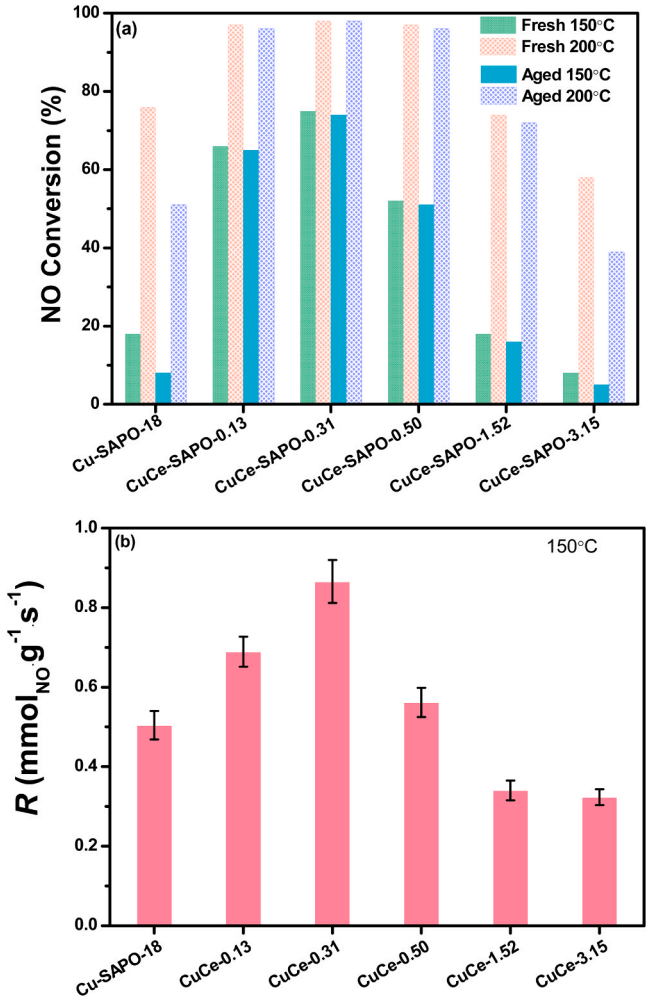

Fig. 22. NH_3-SCR performance of (a) fresh and hydrothermally aged catalysts at 150°C and 200°C, and (b) reaction rates over the fresh catalysts at 150°C. Reprinted from [27] with permission of Elsevier.

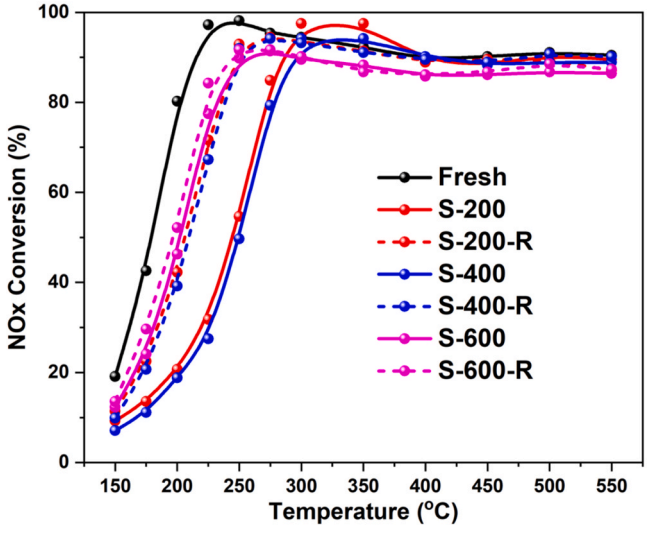

Fig. 23. The catalytic performance of fresh, sulfated and regenerated catalysts. [NO] = [NH_3] = 500 ppm, [O_2] = [H_2O] = 5 vol%, N_2 balance, GHSV = 200 000 h^{-1}. Reprinted from [104] with permission of Royal Society of Chemistry.

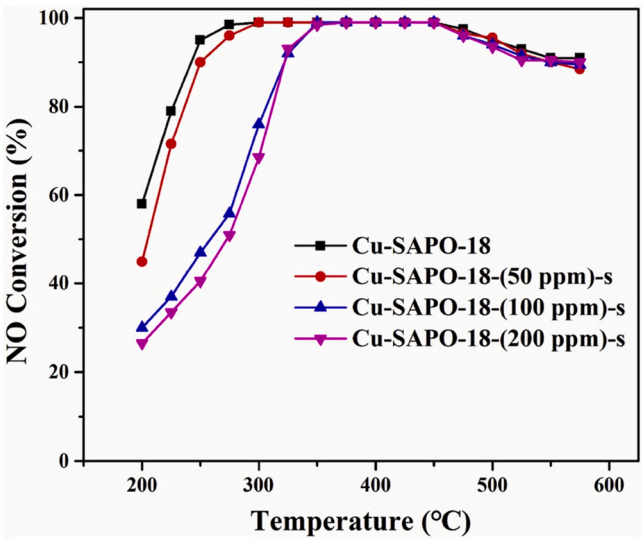

Fig. 24. NH_3-SCR performance of fresh and sulfated Cu-SAPO-18. Reprinted from [95] with permission of Elsevier.

affected, which is due to the fact that even if a portion of Cu^{2+} are poisoned by SO_2 to form stable $CuSO_4$, leaving enough Cu^{2+} active sites for the high-temperature NH_3-SCR reaction due to the high cycling frequency [106]. After regenerating the sulfated catalysts at 550 °C for 1–3 h, respectively, the sulfated catalysts by 50 and 100 ppm SO_2 almost recovered to their original activities. Whereas the activity of the sulfated catalyst by 200 ppm SO_2 cannot be recovered to the initial level below 300 °C. Even the regeneration time was prolonged to 2 and 3 h, there is still about 15% and 10% activity loss at 200 °C. At 550 °C the unstable sulfide on the catalyst surface can be removed, and the stable copper sulfate can be eliminated by redox cycling between Cu(II) and Cu(I) induced by NO + NH_3 [107]. However, only some Cu(II) sites can interact with "NO+ NH_3", which accounts for the partial recovery of the activity after the regeneration [107].

Based on the in situ DRIFTS analysis, Ming et al.[95]. proposed an NH_3-SCR reaction pathway for Cu-SAPO-18 catalysts before and after sulfation. As shown in Fig. 25, the NH_3-SCR reaction on the Cu-SAPO-18 catalyst followed the "L-H" mechanism. The presence of NO_3^- and NO_2^- species on the surface of Cu-SAPO-18 is recognized to enhance its low-temperature activity. Nevertheless, when Cu-SAPO-18 is exposed to

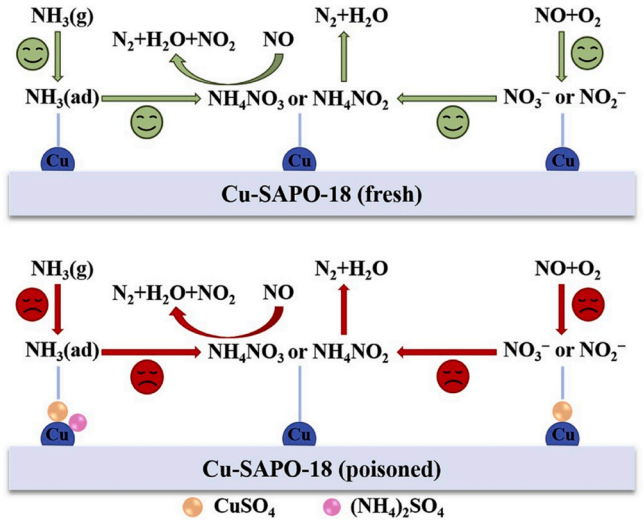

Fig. 25. The deactivation mechanism for Cu-SAPO-18 catalyzed NH_3-SCR caused by SO_2. Reprinted from [95] with permission of Elsevier.

SO_2, the formation of $CuSO_4$ species occurs, impeding the adsorption of NH_3 and NO_x species on Cu^{2+}. Sulfate species formed on the Cu-SAPO-18 also react with NH_3 to form $(NH_4)_2SO_4$ species, which would cover the active Cu^{2+} sites. And NH_3 is readily oxidized to NO_2 and NH_2 in the presence of SO_4^{2-}, reducing the adsorption of NH_3 species. Therefore, the predominant "L-H" mechanism over the sulfated catalyst is restricted. At the same time, NH_2 can react with NO to form NH_2NO through the "E-R" mechanism, which further dissociates into N_2 and H_2O. However, the "L-H" mechanism on sulfated catalysts is still faster than the accelerated "E-R" mechanism, which could account for the decreased low-temperature NH_3-SCR activity of the sulfate catalyst.

6.2. Phosphorus poisoning

Phosphorus poisoning is also a noteworthy issue in the NH_3-SCR reaction. The phosphorus contaminant primarily arises from the combustion of biomass fuel and engine lubricating oil additives, such as Zinc Dialkyl Dithiophosphate (ZDDP) and alkyl polyphosphates[108].

In the case of Cu-SSZ-39 catalysts, Chen et al.[109] found that the presence of P led to a significant decrease of the NH_3-SCR activity, and the inhibiting effect becomes more serious with increasing the content of P. The formation of Cu-P species, which led to a decrease in the redox ability of the active copper species, can account for the decreased activity. For Cu-SSZ-13 catalyst, the NH_3-SCR activity was also suppressed by phosphorus, and the activity was totally lost at 350 °C [110]. Lezcano-Gonzalez et al. [110] proposed that the deposition of polyphosphate covering the active sites, the disruption of the zeolite framework induced by phosphorus, and the loss of active sites due to the formation of CuO, are responsible for the deactivation.

Interestingly, the activity loss of P-poisoned Cu-SSZ-39 can be alleviated by further hydrothermal aging treatment at 800 °C, during which the Cu-P species can be partially decomposed with the formation of active CuO_x species and a release of active copper species. As a result, even for the most seriously poisoned Cu-SSZ-39 catalyst, after the hydrothermal treatment, over 95% NO_x conversion can be achieved at 250 °C (Fig. 26) [109]. In contrast, Xie et al.[108] reported that the hydrothermal aging led to a significant decrease in the SCR activity of P-poisoned Cu-SSZ-13 catalyst, and proposed that the hydrothermal aging process resulted in the formation of $AlPO_4$, which accelerated the dealumination process of the skeleton. To date, little research about the effect of P on Cu-SAPO-18 catalyst has been reported. Therefore, intensive study on this catalyst is needed.

6.3. Alkali metal poisoning

In the diesel exhaust, various alkali and alkaline earth metals (K, Na, Ca and Mg) coming from the urea solutions and engine lubricating oils [10,111,112] are considered to be chemically toxic to SCR catalysts. Their effects on catalyst activity are mainly manifested as follows: (1) Alkali or alkaline earth metals can deposit on the catalyst surface and block the catalyst pores, causing the neutralization of Brönsted acid sites, thus reducing the adsorption of NH_3 and strongly affecting the catalytic performance[113,114]. (2) These metals will react with the acidic gases in the exhaust to produce insoluble substances, such as $CaSO_4$[115], which will be deposited on the catalyst surface and cover the active sites, thus leading to the decreased activity.

6.3.1. Plugging of pores and decreased acid sites

Considering that the diameters of Mg^{2+} (1.44 Å), Ca^{2+} (2.00 Å), Na^+ (2.04 Å) and K^+ (2.76 Å) are smaller than the pore diameters of SSZ-39 and SAPO-18 zeolites (3.8 Å). These alkali metal ions may enter into the zeolite pore channels, leading to a significant decrease of the catalyst specific surface area and pore volume. It may also cause the catalyst micropores to be plugged, or the zeolite structure may be partially destroyed [116,117]. Moreover, the number and strength of acid sites on the surface of the catalyst will be reduced[116,117], thus decreasing the adsorption of NH_3. Gao et al.[118] reported that after introducing Ca into the Cu-SAPO-18 catalyst, Ca^{2+} can replace H^+ or Cu^{2+} in the Si-O (H) -Al or Si-O (Cu^{2+}) -Al to form Si-O (Ca^{2+}) -Al species, resulting in significant decrease of Lewis acid and Brönsted acid sites, which is a crucial reason for the decreased SCR activity. Ming et al.[117] reported that the ionic diameter and basic strength of the alkali metals is related to the deactivation degree of the catalyst. After the introduction of K, Na, Ca and Mg into Cu-SAPO-18, these metal ions with different hydrated ion diameters replaced H^+ or Cu^{2+} to different degrees, resulting in the reduction of both Cu^{2+} species and acidic sites of the catalyst. Moreover,

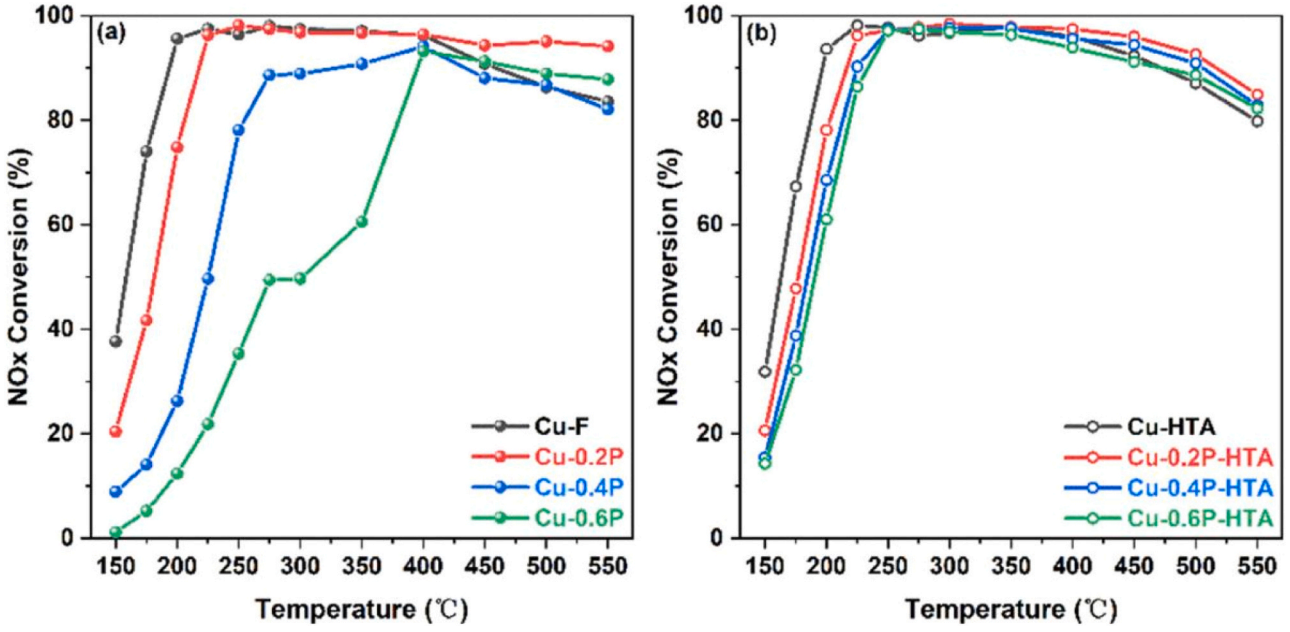

Fig. 26. NO_x conversion of fresh and phosphorus-poisoned Cu-SSZ-39 catalysts before (a) and after (b) hydrothermal aging treatment. The inlets consisted of 500 ppm NO, 500 ppm NH_3, 5% O_2, and 5% H_2O and were balanced by N_2, GHSV = 100,000 h^{-1}. Reprinted from [109] with permission of American Chemical Society.

Cu^{2+} was converted into CuO species and $CuAl_2O_4$ species during the high-temperature calcination, which led to the micropores plugging of Cu-SAPO-18 catalyst as well as the covering of the acid sites. The decrease of the overall acid sites over Cu/M-SAPO-18(x) follows the order of Cu/K>Cu/Na>Cu/Ca>Cu/Mg-SAPO-18(x). Although two K^+ or Na^+ can replace two H^+ or one Cu^{2+}, and one Ca^{2+} or Mg^{2+} can replace two H^+ or one Cu^{2+}, the small hydration diameters of K^+ and Na^+ are more accessible to the small-pore Cu-SAPO-18 catalyst than Ca^{2+} and Mg^{2+}. Thus, a large number of Brönsted acid sites and isolated Cu^{2+} are more readily exchanged with K^+ and Na^+, leading to a more significant decrease of the total acid sites over Cu/K-SAPO-18 and Cu/Na-SAPO-18 catalysts.

The same pattern can also be found in the case of Cu-SSZ-39 catalyst [106]. K/Cu-SSZ-39 possesses the weakest acid sites, Na^+ is of the second highest effect on the acid sites, and Ca and Mg exert little effect on the acidity of this catalyst. The amount of acid sites was decreased in the order of Cu-SSZ-39 > Mg/Cu-SSZ-39 > Ca/Cu-SSZ-39 > Na/Cu-SSZ39 > K/Cu-SSZ-39, which was not consistent with the activity sequence of these catalysts. Accordingly, in addition to the catalyst structure and acid sites, it is still necessary to investigate the effects of other factors on the activity.

6.3.2. Loss of Cu active site

It is generally recognized that Cu^{2+} is the active site for the NH_3-SCR reaction[119]. Therefore, the conversion of isolated Cu^{2+} to CuO_x species seems to be a significant factor for the deactivation of Cu-AEI catalyst by alkali/alkaline metal poisoning. Gao et al.[118,120] reported that the amount of isolated Cu^{2+} on Cu-SAPO-18 catalyst was decreased dramatically (from 62.83 μmol/g to 23.45 μmol/g) due to the Ca poisoning, and they found that the isolated Cu^{2+} species was converted to Cu_2O after the addition of Ca. Ca ions can enter the 8MR and D6R of the catalyst, covering part of the active sites, which in turn leads to a decreased activity [120]. Zhu et al.[116] demonstrated that the poisoning effects of alkaline earth metals on Cu-SSZ-39 were decreased in the order of K > Mg > Ca > Na. The loss of the acid sites, the formation of CuO_x and $CuAlO_x$ from isolated Cu^{2+} induced by alkali metals/alkaline earth metals are mainly responsible for the decrease of the NH_3-SCR activity [85,121]. Fig. 27 shows the relative number of acid sites (based on NH_3-TPD results) and the isolated Cu^{2+} (based on EPR results) as a function of the actual metal content. Cu^{2+} content in Cu/M-SAPO-18(x) catalyst is decreased in the order of Cu/Na>Cu/K>Cu/Mg>Cu/Ca-SAPO-18(x). The acid sites are decreased in the order of Cu/K>Cu/Na>Cu/Ca>Cu/Mg-SAPO-18(x), corresponding to the degree of catalysts deactivation. The separated Cu^{2+}, catalyst structure and acid sites can collectively affect the SCR activity of the catalyst.

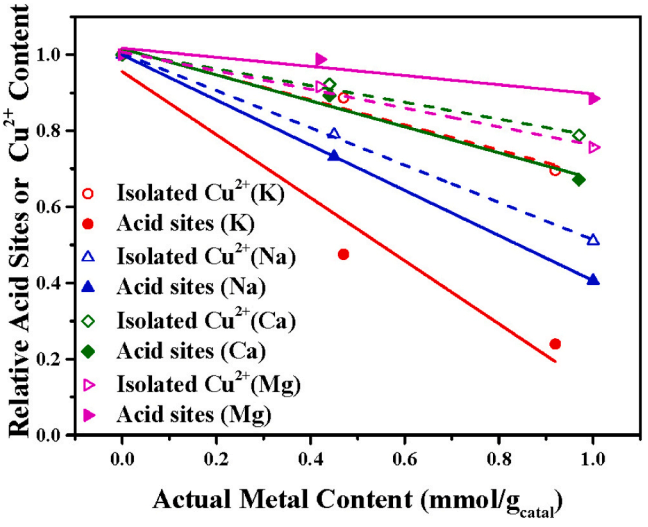

Fig. 27. The relative content of acid sites (according to the NH_3-TPD results) and the relative number of isolated Cu^{2+} ions (according to the EPR results) as a function of actual metal ion content. Reprinted from [117] with permission of Elsevier.

The effects of the alkali metals on the NH_3-SCR mechanism over Cu-SAPO-18 catalyst were investigated by the kinetic studies at low temperatures. All the catalysts have similar apparent activation energies, indicating that the presence of K, Na, Ca, and Mg on Cu-SAPO-18 exerts little effect on the NH_3-SCR mechanism [117].

6.4. HC poisoning

The presence of HC in the exhaust can affect the activity of Cu-zeolite catalyst. Especially during the cold start or long idling the unconverted HC will be emitted and exert impact on the NH_3-SCR activity of the catalyst [122,123]. Zhang et al.[124] reported that in the NH_3-SCR reaction the presence of propene can result in a decrease of the activity due to the coke deposition. On one hand, coke deposition led to the decrease of the surface area and pore volume of the zeolite. The tolerance of the catalyst to HC poisoning depends on the pore structure of the zeolites. Zeolites with pore size larger than the kinetic diameter of propene molecule (~ 4.5 Å) are favorable for the effective diffusion of propene, and the coke deposition can be formed on their pores and external surface. If the pore size of the zeolite is smaller than the kinetic diameter of propene, the direct entering of propene to the pores can be inhibited, and the coke deposition occurs only on its external surface. On the other hand, since hydrocarbons are most active on the acid sites, the extent of coke deposition is related to the acidity of zeolite. In addition, hydrocarbon combustion at high temperatures can release some heat, which can damage the skeleton structure of zeolite. Ye et al. [125] successfully synthesized SAPO-18 using N, N-diisopropylethylamine as a structure directing agent and found that Cu-SAPO-18 showed high SCR activity, hydrothermal stability, and resistance against propene poisoning (Fig. 28). Its activity is seldom affected in the low(< 250 °C) and high(> 400 °C) temperature range. The NO_x conversion was decreased only between 250 and 400 °C. Cu-SAPO-18 exhibited higher tolerance to propene than Cu-ZSM-5 catalyst. Characterization showed that less deposited coke was formed over Cu-SAPO-18 than Cu-ZSM-5 during the reaction in the presence of propene. Even after SCR with 700 ppm propene at 250 °C for 10 h, both the surface area and pore volume of Cu/SAPO-18 catalyst hardly changed, indicating this catalyst is of high tolerance to propene.

At present, propene was usually used to investigate the effect of HC on the catalytic performance of Cu-zeolite catalyst. Since in the actual exhaust different hydrocarbons are present [123,126,127], in order to better evaluate the HC-resistant ability of Cu-AEI catalyst, further study should be conducted using different types of HC, such as light alkanes and alkenes.

7. Comparison between Cu-SSZ-39 and Cu-SAPO-18

Both SSZ-39 and SAPO-18 zeolites are of the same AEI topology. The high activity and excellent hydrothermal stability demonstrated that the Cu-AEI zeolite catalyst has a high potential for the application in the NH_3-SCR of NO_x. However, there are still some differences in terms of SCR activity and hydrothermal stability.

For Cu-SSZ-39 catalyst, as the Cu loading is increased from 1.5% to 2.5%, the activity is seldom changed and the NO_x conversion is about 68% at 200 °C. The SCR activities of $Cu_{1.5}$-SSZ-39 and $Cu_{2.5}$-SSZ-39 showed almost identical activities below 400 °C, but the NO_x conversion over $Cu_{2.5}$-SSZ-39 is decreased above 400 °C, which could be due to the increase of CuO_x species [21]. In the case of Cu-SAPO-18 catalyst, the effect of Cu content on the activity is more noticeable. The activity is enhanced obviously with increasing the Cu loading from 1.53% to

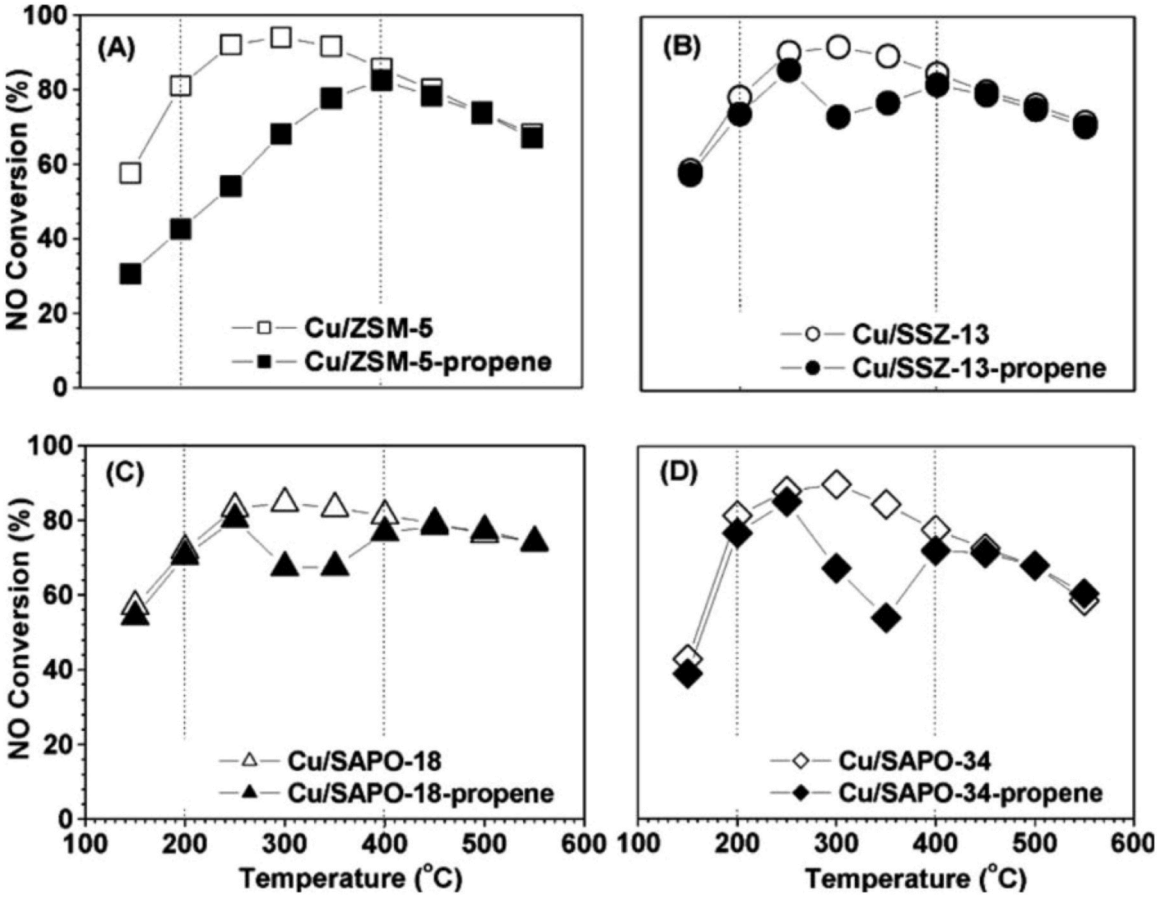

Fig. 28. Catalytic activities for SCR of NO by NH_3 over (A) Cu/ZSM-5; (B) Cu/SSZ-13; (C) Cu/SAPO-18 and (D) Cu/SAPO-34. Reaction conditions: 150 mg catalyst; 400 ppm NO, 400 ppm NH_3, 700 ppm C_3H_6 (when used), 14% O_2, 2% H_2O and He as balance. Total flow rate 300 mL/min. Reprinted from [125] with permission of Elsevier.

2.49%, and the NO conversion at 200 °C is increased from about 52% to 70%. NO conversion of $Cu_{2.49}$-SAPO-18 was significantly higher than that of $Cu_{1.53}$-SAPO-18 in the temperature range of 200–550 ℃ [59]. The lack of sufficient active isolated Cu^{2+} could account for the inferior activity of $Cu_{1.53}$-SAPO-18 catalyst.

After the hydrothermal treatment at 750 °C, the NH_3-SCR activity of $Cu_{2.49}$-SAPO-18 catalyst is decreased slightly due to the less decrease of isolated Cu^{2+} species. But a significant decrease of NH_3-SCR activity is observed for $Cu_{3.51}$-SAPO-18 catalyst [59]. For the latter catalyst, the deactivation is due to the formed CuO species, which can cause some damage to its framework [128,129]. Unlike the Cu-SAPO-18 catalyst, Du et al.[130] reported that the activities of Cu-SSZ-39 catalysts with suitable Cu contents (1.3–2.0 wt%) were increased instead after the hydrothermal aging treatment at 850 °C for 16 h. They attributed the activity enhancement to the conversion of some Cu^{2+} to Cu_xO_y, which acts as the new active sites. The Cu_xO_y species can promote the formation of nitrate species, a key intermediate in the SCR process, thus leading to an unexpected enhancement of its SCR activity. The discrepancies between Cu-SSZ-39 and Cu-SAPO-18 upon the catalytic performance are still not clear. Therefore, comparative studies of these two catalysts are desirable.

8. Conclusions and perspectives

In this review, selective catalytic reduction of NO_x by NH_3 over Cu-AEI zeolite catalyst has been systematically summarized in terms of the NH_3-SCR reaction mechanism, synthesis method, hydrothermal stability, and catalyst deactivation. The strategies to improve its low temperature activity, hydrothermal stability and protection against poisoning by modifying the Cu active site during the synthesis and post-treatment are further discussed, which can help researchers get a comprehensive understanding of the Cu-AEI zeolite catalyst for the NH_3-SCR of NO_x.

Compared with other Cu-based zeolite catalysts, the Cu-AEI catalyst exhibits excellent hydrothermal stability due to its particular pore structure and small pore size that limits the diffusion of skeletal aluminum and the accumulation of Cu species during the hydrothermal process. This makes it a potential candidate for the removal of NO_x under severe diesel exhaust environment. However, several challenges need to be overcome to expand its application in the NH_3-SCR reaction:

(1) Exploring green and economical synthesis routes for AEI zeolite is essential for their practical application. Although some environmentally benign methods for the synthesis of Cu-AEI zeolite have been reported, the complex preparation procedure as well as the high cost of the catalyst limits its commercial application. Based on the deep understanding of the relationship between the structure and the catalytic performance would guide the optimizing of the synthesis conditions, and developing more simple and economical preparation method to reduce the cost and achieve large-scale production.

(2) In the actual diesel exhaust, the gas composition is complex, leading to the complicated effect on the catalytic performance of the AEI zeolite. At present, most of the research was focused on the deactivation of catalyst in the presence of only one poisonous substance. In the case of the presence of more substances, the individual factors could interact with each other, such as the offset or synergetic effect. However, the effects of the

simultaneous existence of multiple substances are not clear yet. Therefore, the research on the co-effects of multiple elements should be investigated in the future research, which would be more important for the exploring of anti-deactivation strategy and promoting the stability of the Cu-AEI zeolite.

(3) Besides the fabrication of the precise structure of the AEI zeolite, it is still necessary to further investigate the NH_3-SCR reaction mechanism as well as the deactivation mechanism of AEI zeolite in more detail. The combination of in-situ X-ray absorption spectroscopy (XAFS), in-situ Diffuse Reflectance Infrared Fourier Transform Spectroscopy (DRIFTS), and the density functional theory (DFT) calculations should be a powerful tool to uncover the role of different active sites as well as the pore structure, the reactivity of the reaction intermediates and the reaction routes, all of which are conducive for the design of more efficient Cu-AEI zeolite catalyst.

Declaration of Competing Interest

The authors declare that they have no known competing financial interests or personal relationships that could have appeared to influence the work reported in this paper.

Data Availability

Data will be made available on request.

Acknowledgments

The authors acknowledge financial support from the National Natural Science Foundation of China (22276010, 22211530066, 21876009), and the Fundamental Research Funds for the Central Universities (JD2110).

References

[1] L. Han, S. Cai, M. Gao, J.Y. Hasegawa, P. Wang, J. Zhang, L. Shi, D. Zhang, Selective catalytic reduction of NO_x with NH_3 by using novel catalysts: state of the art and future prospects, Chem. Rev. 119 (2019) 10916–10976, https://doi.org/10.1021/acs.chemrev.9b00202.

[2] G. Busca, L. Lietti, G. Ramis, F. Berti, Chemical and mechanistic aspects of the selective catalytic reduction of NOx by ammonia over oxide catalysts: a review, Appl. Catal. B-Environ. 18 (1–2) (1998) 1–36, https://doi.org/10.1016/S0926-3373(98)00040-X.

[3] J. Li, H. Chang, L. Ma, J. Hao, R.T. Yang, Low-temperature selective catalytic reduction of NO_x with NH_3 over metal oxide and zeolite catalysts-a review, Catal. Today 175 (2011) 147–156, https://doi.org/10.1016/j.cattod.2011.03.034.

[4] Q. Sun, Z. Xie, J. Yu, The state-of-the-art synthetic strategies for SAPO-34 zeolite catalysts in methanol-to-olefin conversion, Natl. Sci. Rev. 5 (2017) 542–588, https://doi.org/10.1093/nsr/nwx103.

[5] Z. Xie, Z. Liu, Y. Wang, Z. Jin, Applied catalysis for sustainable development of chemical industry in China, Natl. Sci. Rev. 2 (2015) 167–182, https://doi.org/10.1093/nsr/nwv019.

[6] R. Zhang, N. Liu, Z. Lei, B. Chen, Selective transformation of various Nitrogen-Containing exhaust gases toward N_2 over zeolite catalysts, Chem. Rev. 116 (2016) 3658, https://doi.org/10.1021/acs.chemrev.5b00474.

[7] J.H. Kwak, R.G. Tonkyn, D.H. Kim, J. Szanyi, C. Peden, Excellent activity and selectivity of Cu-SSZ-13 in the selective catalytic reduction of NO_x with NH_3, J. Catal. 275 (2010) 187–190, https://doi.org/10.1016/j.jcat.2010.07.031.

[8] D.W. Fickel, E. D'Addio, J.A. Lauterbach, R.F. Lobo, The ammonia selective catalytic reduction activity of copper-exchanged small-pore zeolites, Appl. Catal. B-Environ. 102 (2011) 441–448, https://doi.org/10.1016/j.apcatb.2010.12.022.

[9] I. Bull, W.M. Xue, P. Burk, R.S. Boorse, W.M. Jaglowski, G.S. Koermer, A. Moini, J.A. Patchett, J.C. Dettling, M.T. Caudle, Copper CHA zeolite catalysts, United States Patent 7601662.

[10] J.H. Kwak, D. Tran, S.D. Burton, J. Szanyi, J.H. Lee, C.H.F. Peden, Effects of hydrothermal aging on NH_3-SCR reaction over Cu/zeolites, J. Catal. 287 (2012) 203–209, https://doi.org/10.1016/j.jcat.2012.02.009.

[11] K. Leistner, A. Kumar, K. Kamasamudram, L. Olsson, Mechanistic study of hydrothermally aged Cu/SSZ-13 catalysts for ammonia-SCR, Catal. Today 307 (2017) 55–64, https://doi.org/10.1016/j.cattod.2017.04.015.

[12] X.Y. Zhang, T.T. Dou, Y. Wang, J.Y. Yang, X. Wang, Y.Y. Guo, Q. Shen, X. Zhang, S.Q. Zhang, Green synthesis of Cu-SSZ-13 zeolite by seed-assisted route for effective reduction of nitric oxide, J. Clean. Prod. 236 (2019) 117667, https://doi.org/10.1016/j.jclepro.2019.117667.

[13] N.H. Ahn, T. Ryu, Y. Kang, H. Kim, J. Shin, I.S. Nam, S.B. Hong, The origin of an unexpected increase in NH_3-SCR activity of aged Cu-LTA catalysts, ACS Catal. 7 (2017) 6781–6785, https://doi.org/10.1021/acscatal.7b02852.

[14] J. Lin, X. Hu, Y. Li, W. Shan, X. Tan, H. He, Maximizing the hydrothermal stability of Cu-LTA for NH_3-SCR by control of Cu content and location, Appl. Catal. B-Environ. 331 (2023), 122705, https://doi.org/10.1016/j.apcatb.2023.122705.

[15] J. Wang, H. Zhao, G. Haller, Y. Li, Recent advances in the selective catalytic reduction of NO_x with NH_3 on Cu-Chabazite catalysts, Appl. Catal. B-Environ. 202 (2017) 346–354, https://doi.org/10.1016/j.apcatb.2016.09.024.

[16] E. Borfecchia, P. Beato, S. Svelle, U. Olsbye, C. Lamberti, S. Bordiga, Cu-CHA - a model system for applied selective redox catalysis, Chem. Soc. Rev. 47 (2018) 8097–8133, https://doi.org/10.1039/c8cs00373d.

[17] P. Li, Y. Xin, H. Zhang, F. Yang, A. Tang, D. Han, J. Jia, J. Wang, Z. Li, Z. Zhang, Recent progress in performance optimization of Cu-SSZ-13 catalyst for selective catalytic reduction of NO_x, Front. Chem. 10 (2022), 1033255, https://doi.org/10.3389/fchem.2022.1033255.

[18] S. Zhang, L. Pang, Z. Chen, S. Ming, Y. Dong, Q. Liu, P. Liu, W. Cai, T. Li, Cu/SSZ-13 and Cu/SAPO-34 catalysts for deNO_x in diesel exhaust: current status, challenges, and future perspectives, Appl. Catal. A-Gen. 607 (2020) 117855, https://doi.org/10.1016/j.apcata.2020.117855.

[19] S. Mohan, P. Dinesha, S. Kumar, NO_x reduction behaviour in copper zeolite catalysts for ammonia SCR systems: a review, Chem. Eng. J. 384 (2020) 123253, https://doi.org/10.1016/j.cej.2019.123253.

[20] Y. Shan, J. Du, Y. Zhang, W. Shan, X. Shi, Y. Yu, R. Zhang, X. Meng, F.S. Xiao, H. He, Selective catalytic reduction of NO_x with NH_3: opportunities and challenges of Cu-based small-pore zeolites, Natl. Sci. Rev. 8 (2021), nwab010, https://doi.org/10.1093/nsr/nwab010.

[21] G. Fu, R. Yang, Y. Liang, X. Yi, R. Li, N. Yan, A. Zheng, L. Yu, X. Yang, J. Jiang, Enhanced hydrothermal stability of Cu/SSZ-39 with increasing Cu contents, and the mechanism of selective catalytic reduction of NO, Microporous Mesoporous Mat. 320 (2021), 111060, https://doi.org/10.1016/j.micromeso.2021.111060.

[22] N. Zhu, Y. Shan, W. Shan, Z. Lian, J. Du, H. He, Reaction pathways of standard and fast selective catalytic reduction over Cu-SSZ-39, Environ. Sci. Technol. 55 (2021) 16175–16183, https://doi.org/10.1021/acs.est.1c06475.

[23] M.P. Ruggeri, I. Nova, E. Tronconi, J.A. Pihl, W.P. Partridge, In-situ DRIFTS measurements for the mechanistic study of NO oxidation over a commercial Cu-CHA catalyst, Appl. Catal. B-Environ. 166–167 (2015) 181–192, https://doi.org/10.1016/j.apcatb.2014.10.076.

[24] Q. Lin, S. Xu, H. Zhao, S. Liu, H. Xu, Y. Dan, Y. Chen, Highlights on key roles of Y on the hydrothermal stability at 900°C of Cu/SSZ-39 for NH_3-SCR, ACS Catal. 12 (2022) 14026–14039, https://doi.org/10.1021/acscatal.2c03757.

[25] Y. Wang, G.G. Li, S.Q. Zhang, X.Y. Zhang, X. Zhang, Z.P. Hao, Promoting effect of Ce and Mn addition on Cu-SSZ-39 zeolites for NH_3-SCR reaction: activity, hydrothermal stability, and mechanism study, Chem. Eng. J. 393 (2020) 124782, https://doi.org/10.1016/j.cej.2020.124782.

[26] Y. Li, J. Deng, W. Song, J. Liu, Z. Zhao, M. Gao, Y. Wei, L. Zhao, Nature of Cu species in Cu–SAPO-18 catalyst for NH_3–SCR: combination of experiments and DFT calculations, J. Phys. Chem. C. 120 (2016) 14669–14680, https://doi.org/10.1021/acs.jpcc.6b03464.

[27] Q. Wu, C. Fan, Y. Wang, X. Chen, G. Wang, Z. Qin, S. Mintova, J. Li, J. Chen, Direct incorporating small amount of Ce (III) in Cu-SAPO-18 catalysts for enhanced low-temperature NH_3-SCR activity: Influence on Cu distribution and Si coordination, Chem. Eng. J. 435 (2022) 134890, https://doi.org/10.1016/j.cej.2022.134890.

[28] S. Ming, S. Zhang, K. Qin, P. Liu, Y. Guo, L. Pang, T. Li, Promoting effect of post-synthesis treatment strategy on NH_3-SCR performance and hydrothermal stability of Cu-SAPO-18, Micro Mesopor. Mat. 328 (2021) 111496, https://doi.org/10.1016/j.micromeso.2021.111496.

[29] M. Moliner, C. Franch, E. Palomares, M. Grill, A. Corma, Cu-SSZ-39, an active and hydrothermally stable catalyst for the selective catalytic reduction of NO_x, Chem. Commun. 48 (2012) 8264–8266, https://doi.org/10.1039/c2cc33992g.

[30] M. Dusselier, J.E. Schmidt, R. Moulton, B. Haymore, M. Hellums, M.E. Davis, Influence of organic structure directing agent isomer distribution on the synthesis of SSZ-39, Chem. Mater. 27 (7) (2015) 2695–2702, https://doi.org/10.1021/acs.chemmater.5b00651.

[31] M. Dusselier, M.A. Deimund, J.E. Schmidt, M.E. Davis, Methanol-to-Olefins catalysis with hydrothermally treated zeolite SSZ-39, ACS Catal. 5 (10) (2015) 6078–6085, https://doi.org/10.1021/acscatal.5b01577.

[32] R. Ransom, J. Coote, R. Moulton, F. Gao, D.F. Shantz, Synthesis and growth kinetics of zeolite SSZ-39, Ind. Eng. Chem. Res. 56 (2017) 4350–4356, https://doi.org/10.1021/acs.iecr.7b00629.

[33] J. Zhang, N. Wu, A. Tong, Y. Liu, Structural dynamic responses of a stripped solar sail subjected to solar radiation pressure, Chin. J. Aeronaut. 33 (2020) 2204–2211, https://doi.org/10.1021/10.1016/j.cja.2020.05.003.

[34] N. Martin, Z. Li, J. Martinez-Triguero, J. Yu, M. Moliner, A. Corma, Nanocrystalline SSZ-39 zeolite as an efficient catalyst for the methanol-to-olefin (MTO) process, Chem. Commun. 52 (2016) 6072–6075, https://doi.org/10.1039/c5cc09719c.

[35] S.I. Zones, Y. Nakagawa, S.T. Evans, G.S. Lee, Zeolite SSZ-39, United States Patent 08/988723.

[36] T. Sonoda, T. Maruo, Y. Yamasaki, N. Tsunoji, Y. Takamitsu, M. Sadakane, T. Sano, Synthesis of high-silica AEI zeolites with enhanced thermal stability by hydrothermal conversion of FAU zeolites, and their activity in the selective catalytic reduction of NO_x with NH_3, J. Mater. Chem. A. 3 (2015) 857–865, https://doi.org/10.1039/c4ta05621c.

[37] K. Itabashi, Y. Kamimura, K. Iyoki, A. Shimojima, T. Okubo, A working hypothesis for broadening framework types of zeolites in seed-assisted synthesis without organic structure-directing agent, J. Am. Chem. Soc. 134 (2012) 11542–11549, https://doi.org/10.1021/ja3022335.
[38] K. Honda, M. Itakura, Y. Matsuura, A. Onda, Y. Ide, M. Sadakane, T. Sano, Role of structural similarity between starting zeolite and product zeolite in the interzeolite conversion process, J. Nanosci. Nanotechnol. 13 (2013) 3020–3026, https://doi.org/10.1166/jnn.2013.7356.
[39] S. Goel, S.I. Zones, E. Iglesia, Synthesis of zeolites via interzeolite transformations without organic structure-directing agents, Chem. Mater. 27 (2015) 2056–2066, https://doi.org/10.1021/cm504510f.
[40] Q. Wang, S. Xu, J. Chen, Y. Wei, J. Li, D. Fan, Z. Yu, Y. Qi, Y. He, S. Xu, C. Yuan, Y. Zhou, J. Wang, M. Zhang, B. Su, Z. Liu, Synthesis of mesoporous ZSM-5 catalysts using different mesogenous templates and their application in methanol conversion for enhanced catalyst lifespan, RSC Adv. 4 (2014) 21479–21491, https://doi.org/10.1039/c4ra02695k.
[41] L. Zhao, B. Shen, J.C. Gao, Investigation on the mechanism of diffusion in mesopore structured ZSM-5 and improved heavy oil conversion, J. Catal. 258 (1) (2008) 228–234, https://doi.org/10.1016/j.jcat.2008.06.015.
[42] V. Valtchev, L. Tosheva, Porous nanosized particles: preparation, properties, and applications, Chem. Rev. 113 (2013) 6734–6760, https://doi.org/10.1021/cr300439k.
[43] J. Zhang, W. Qian, C. Kong, F. Wei, Increasing para -Xylene selectivity in making aromatics from methanol with a surface-modified Zn/P/ZSM-5 catalyst, ACS Catal. 5 (2015) 2982–2988, https://doi.org/10.1021/acscatal.5b00192.
[44] M. Thommes, S. Mitchell, J. Pérez-Ramírez, Surface and pore structure assessment of hierarchical MFI zeolites by advanced water and argon sorption studies, J. Phys. Chem. C. 116 (2012) 18816–18823, https://doi.org/10.1021/jp3051214.
[45] M. Choi, K. Na, J. Kim, Y. Sakamoto, O. Terasaki, R. Ryoo, Stable single-unit-cell nanosheets of zeolite MFI as active and long-lived catalysts, Nature 461 (7261) (2009) 246–249, https://doi.org/10.1038/nature08288.
[46] H. Xu, W. Chen, Q.M. Wu, C. Lei, J. Zhang, S.C. Han, L. Zhang, Q.Y. Zhu, X. J. Meng, D. Dai, S. Maurer, A.N. Parvulescu, U. Muller, W.P. Zhang, T. Yokoi, X. H. Bao, B. Marler, D.E. De Vos, U. Kolb, A.M. Zheng, F.S. Xiao, Transformation synthesis of aluminosilicate SSZ-39 zeolite from ZSM-5 and beta zeolite, J. Mater. Chem. A. 7 (2019) 4420–4425, https://doi.org/10.1039/c9ta00174c.
[47] J. Zhang, Y.Y. Chu, F. Deng, Z.C. Feng, X.J. Meng, F.S. Xiao, Evolution of D6R units in the interzeolite transformation from FAU, MFI or *BEA into AEI: transfer or reassembly? Inorg. Chem. Front. 7 (2020) 2204, https://doi.org/10.1039/d0qi00359j.
[48] H. Xu, J. Zhu, J. Qiao, X. Yu, N.-B. Sun, C. Bian, J. Li, L. Zhu, Solvent-free synthesis of aluminosilicate SSZ-39 zeolite, Microporous Mesoporous Mat 312 (2021) 110736, https://doi.org/10.1016/j.micromeso.2020.110736.
[49] H. Xu, J. Zhang, Q. Wu, W. Chen, C. Lei, Q. Zhu, S. Han, J. Fei, A. Zheng, L. Zhu, X. Meng, S. Maurer, D. Dai, A.-N. Parvulescu, U. Müller, F.-S. Xiao, Direct synthesis of aluminosilicate SSZ-39 zeolite using colloidal silica as a starting source, ACS Appl. Mater. Interfaces 11 (2019) 23112–23117, https://doi.org/10.1021/acsami.9b03048.
[50] J. Chen, J.M. Thomas, P.A. Wright, R.P. Townsend, Silicoaluminophosphate number eighteen (SAPO-18): a new microporous solid acid catalyst, Catal. Lett. 28 (1994) 241–248, https://doi.org/10.1007/BF00806053.
[51] J. Chen, P.A. Wright, J.M. Thomas, S. Natarajan, L. Marchese, S.M. Bradley, G. Sankar, C. Catlow, P.L. Gai-Boyes, SAPO-18 catalysts and their broensted acid sites, J. Phys. Chem. 98 (1994) 10216–10224, https://doi.org/10.1021/j100091a042.
[52] S. Zhang, J. Chen, Y. Meng, L. Pang, Y. Guo, Z. Luo, Y. Fang, Y. Dong, W. Cai, T. Li, Insight into solid-state ion-exchanged Cu-based zeolite (SSZ-13, SAPO-18, and SAPO-34) catalysts for the NH_3-SCR reaction: The promoting role of NH_4-form zeolite substrates, Appl. Surf. Sci. 571 (2022) 151328, https://doi.org/10.1016/j.apsusc.2021.151328.
[53] R. Martinez-Franco, M. Moliner, A. Corma, Direct synthesis design of Cu-SAPO-18, a very efficient catalyst for the SCR of NO_x, J. Catal. 319 (2014) 36–43, https://doi.org/10.1016/j.jcat.2014.08.005.
[54] V.R. Rani, R. Singh, P. Payra, P.K. Dutta, Existence of colloidal primitive building units exhibiting memory effects in zeolite growth compositions, J. Phys. Chem. B. 108 (2004) 20465–20470, https://doi.org/10.1021/jp046878k.
[55] L. Guo, S. Ming, S. Zhang, Q. Liu, L. Pang, P. Liu, Z. Chen, T. Li, One-Pot synthesis of the Cu-SAPO-18 catalyst using waste mother liquid and its application in the SCR of NO_x with NH_3, Ind. Eng. Chem. Res. 59 (2020) 21275–21285, https://doi.org/10.1021/acs.iecr.0c03826.
[56] N. Martin, C.R. Boruntea, M. Moliner, A. Corma, Efficient synthesis of the Cu-SSZ-39 catalyst for $DeNO_x$ applications, Chem. Commun. 51 (2015) 11030–11033, https://doi.org/10.1039/c5cc03200h.
[57] J.D. Albarracin-Caballero, I. Khurana, J.R. Di Iorio, A.J. Shih, J.E. Schmidt, M. Dusselier, M.E. Davis, A. Yezerets, J.T. Miller, F.H. Ribeiro, R. Gounder, Structural and kinetic changes to small-pore Cu-zeolites after hydrothermal aging treatments and selective catalytic reduction of NO_x with ammonia, React. Chem. Eng. 2 (2017) 168–179, https://doi.org/10.1039/c6re00198j.
[58] N. Martin, P.N.R. Vennestrom, J.R. Thogersen, M. Moliner, A. Corma, Iron-Containing SSZ-39 (AEI) zeolite: an active and stable high-temperature NH_3-SCR catalyst, ChemCatChem 9 (2017) 1754–1757, https://doi.org/10.1002/cctc.201601627.
[59] S. Ming, Z. Chen, C. Fan, L. Pang, W. Guo, K.B. Albert, P. Liu, T. Li, The effect of copper loading and silicon content on catalytic activity and hydrothermal stability of Cu-SAPO-18 catalyst for NH_3-SCR, Appl. Catal. A-Gen. 559 (2018) 47–56, https://doi.org/10.1016/j.apcata.2018.04.008.
[60] Z. Chen, C. Fan, L. Pang, S. Ming, W. Guo, P. Liu, H. Chen, T. Li, One-pot synthesis of high performance Cu-SAPO-18 catalyst for NO reduction by NH_3-SCR: influence of silicon content on the catalytic properties of Cu-SAPO-18, Chem. Eng. J. 348 (2018) 608–617, https://doi.org/10.1016/j.cej.2018.05.033.
[61] Z.Q. Liu, B. Guan, H. Jiang, Y.F. Wei, X.Z. Wu, J.F. Zhou, H. Lin, Z. Huang, Exploring the optimal ratio of elemental components of the Cu/SSZ-13 framework: the reformation of NH_3-SCR properties, New. J. Chem. 46 (2022) 13593–13607, https://doi.org/10.1039/d2nj01132h.
[62] Y. Shan, W. Shan, X. Shi, J. Du, Y. Yu, H. He, A comparative study of the activity and hydrothermal stability of Al-rich Cu-SSZ-39 and Cu-SSZ-13, Appl. Catal. B-Environ. 264 (2020) 118511, https://doi.org/10.1016/j.apcatb.2019.118511.
[63] Q. Gao, Q. Ye, S. Han, S. Cheng, T. Kang, H. Dai, Effects of Cu/Al mass ratio and hydrothermal aging temperature on catalytic performance of Cu/SAPO-18 for the NH_3-SCR of NO in simulated diesel exhaust, Catal. Surv. Asia. 23 (2019) 344–356, https://doi.org/10.1007/s10563-019-09283-3.
[64] F. Gao, E.D. Walter, M. Kollar, Y.L. Wang, J. Szanyi, C.H.F. Peden, Understanding ammonia selective catalytic reduction kinetics over Cu/SSZ-13 from motion of the Cu ions, J. Catal. 319 (2014) 1–14, https://doi.org/10.1016/j.jcat.2014.08.010.
[65] C. Paolucci, A.A. Parekh, I. Khurana, J.R. Di Iorio, H. Li, J.D.A. Caballero, A. J. Shih, T. Anggara, W.N. Delgass, J.T. Miller, F.H. Ribeiro, R. Gounder, W. F. Schneider, Catalysis in a cage: condition-dependent speciation and dynamics of exchanged Cu cations in SSZ-13 zeolites, J. Am. Chem. Soc. 138 (2016) 6028–6048, https://doi.org/10.1021/jacs.6b02651.
[66] R. Villamaina, S.J. Liu, I. Nova, E. Tronconi, M.P. Ruggeri, J. Collier, A. York, D. Thompsett, Speciation of Cu cations in Cu-CHA catalysts for NH_3-SCR: Effects of SiO_2/AlO_3 ratio and Cu-loading investigated by transient response methods, ACS Catal. 9 (2019) 8916–8927, https://doi.org/10.1021/acscatal.9b02578.
[67] S. Zhou, F.S. Tang, H. Wang, S.N. Wang, L.J. Liu, Effect of Cu concentration on the selective catalytic reduction of NO with ammonia for aluminosilicate zeolite SSZ-13 catalysts, J. Phys. Chem. C. 125 (2021) 14675–14680, https://doi.org/10.1021/acs.jpcc.1c04055.
[68] K. Teraishi, M. Ishida, J. Irisawa, M. Kume, Y. Takahashi, T. Nakano, H. Nakamura, A. Miyamoto, Active site structure of Cu/ZSM-5: Computational study, J. Phys. Chem. B. 101 (1997) 8079–8085, https://doi.org/10.1021/jp970957x.
[69] S.M. Seo, W.T. Lim, K. Seff, Crystallographic verification that copper(II) coordinates to four of the oxygen atoms of zeolite 6-Rings. Two single-crystal structures of fully dehydrated, largely Cu^{2+}-exchanged zeolite Y (FAU, Si/Al=1.56), J. Phys. Chem. C. 116 (2012) 963–974, https://doi.org/10.1021/jp209542x.
[70] G.T. Palomino, S. Bordiga, A. Zecchina, G.L. Marra, C. Lamberti, XRD, XAS, and IR characterization of copper-exchanged Y zeolite, J. Phys. Chem. C. 104 (2000) 8641–8651, https://doi.org/10.1021/jp000584r.
[71] W. Zheng, J.L. Chen, L. Guo, W.B. Zhang, X.Q. Wu, Research progress of hydrothermal stability of metal-based zeolite catalysts in NH_3-SCR reaction, J. Fuel Chem. Technol. 48 (2020) 1193–1210, https://doi.org/10.1016/S1872-5813(20)30081-5.
[72] Z.H. Wang, X. Xu, Y.X. Zhu, H. He, N.L. Wang, X.B. Yang, L.C. Liu, One-pot synthesis of hierarchical MnCu-SSZ-13 catalyst with excellent NH_3-SCR activity at low temperatures, Microporous Mesoporous Mat. 333 (2022) 111720, https://doi.org/10.1016/j.micromeso.2022.111720.
[73] Q. Gao, S. Han, Q. Ye, S. Cheng, T. Kang, H. Dai, Effects of lanthanide doping on the catalytic activity and hydrothermal stability of Cu-SAPO-18 for the catalytic removal of NO_x (NH_3-SCR) from diesel engines, Catalysts 10 (2020) 336, https://doi.org/10.3390/catal10030336.
[74] E.V. Steen, L.H. Callanan, M. Claeys, Recent advances in the science and technology of zeolites and rel, S. Afr. Theatre J. 7 (2004) 101–104, https://doi.org/10.1080/10137548.1993.9688096.
[75] L. Ma, Y. Cheng, G. Cavataio, R.W. Mccabe, L. Fu, J. Li, In situ DRIFTS and temperature-programmed technology study on NH_3-SCR of NO_x over Cu-SSZ-13 and Cu-SAPO-34 catalysts, Appl. Catal. B-Environ. 156–157 (2014) 428–437, https://doi.org/10.1016/j.apcatb.2014.03.048.
[76] M. Pereira, A. Nicolle, D. Berthout, Hydrothermal aging effects on Cu-zeolite NH_3-SCR catalyst, Catal. Today 258 (2015) 424–431, https://doi.org/10.1016/j.cattod.2015.03.027.
[77] L.R. Aramburo, L. Karwacki, P. Cubillas, S. Asahina, D.A.M. de Winter, M. R. Drury, I.L.C. Buurmans, E. Stavitski, D. Mores, M. Daturi, P. Bazin, P. Dumas, F. Thibault-Starzyk, J.A. Post, M.W. Anderson, O. Terasaki, B.M. Weckhuysen, The porosity, acidity, and reactivity of dealuminated zeolite ZSM-5 at the single particle level: The influence of the zeolite architecture, Chem. -A. Eur. J. 17 (2011) 13773–13781, https://doi.org/10.1002/chem.201101361.
[78] T. Sano, H. Ikeya, T. Kasuno, Z.B. Wang, K. Soga, Influence of crystallinity of H-ZSM-5 zeolite on its dealumination rate, Zeolites 19 (1997) 80–86, https://doi.org/10.1016/S0144-2449(97)00052-3.
[79] J.H. Kwak, D. Tran, S.D. Burton, J. Szanyi, J.H. Lee, C.H.F. Peden, Effects of hydrothermal aging on NH_3-SCR reaction over Cu/zeolites, J. Catal. 287 (2012) 203–209, https://doi.org/10.1016/j.jcat.2012.02.009.
[80] P.G. Blakeman, E.M. Burkholder, H.Y. Chen, J.E. Collier, J.M. Fedeyko, H. Jobson, R.R. Rajaram, The role of pore size on the thermal stability of zeolite supported Cu SCR catalysts, Catal. Today 231 (2014) 56–63, https://doi.org/10.1016/j.cattod.2013.10.047.
[81] J. Song, Y. Wang, E.D. Walter, N.M. Washton, F. Gao, Toward rational design of Cu/SSZ-13 selective catalytic reduction catalysts: Implications from atomic-level

understanding of hydrothermal stability, ACS Catal 7 (2017) 8214–8227, https://doi.org/10.1021/acscatal.7b03020.
[82] Y.J. Kim, J.K. Lee, K.M. Min, S.B. Hong, B.K. Cho, Hydrothermal stability of CuSSZ13 for reducing NO_x by NH_3, J. Catal. 311 (2014) 447–457, https://doi.org/10.1016/j.jcat.2013.12.012.
[83] Y.L. Shan, J.P. Du, Y.B. Yu, W.P. Shan, X.Y. Shi, H. He, Precise control of post-treatment significantly increases hydrothermal stability of in-situ synthesized cu-zeolites for NH_3-SCR reaction, Appl. Catal. B-Environ. 266 (2020) 118655, https://doi.org/10.1016/j.apcatb.2020.118655.
[84] F. Gao, E.D. Walter, N.M. Washton, J. Szanyi, C.H.F. Peden, Synthesis and evaluation of Cu/SAPO-34 catalysts for NH_3-SCR 2: Solid-state ion exchange and one-pot synthesis, Appl. Catal. B-Environ. 162 (2015) 501–514, https://doi.org/10.1016/j.apcatb.2014.07.029.
[85] P.N.R. Vennestrom, T.V.W. Janssens, A. Kustov, M. Grill, A. Puig-Molina, L. F. Lundegaard, R.R. Tiruvalam, P. Concepcion, A. Corma, Influence of lattice stability on hydrothermal deactivation of Cu-ZSM-5 and Cu-IM-5 zeolites for selective catalytic reduction of NO_x by NH_3, J. Catal. 309 (2014) 477–490, https://doi.org/10.1016/j.jcat.2013.10.017.
[86] Z.C. Zhao, R. Yu, C. Shi, H. Gies, F.S. Xiao, D. De Vos, T. Yokoi, X.H. Bao, U. Kolb, R. McGuire, A.N. Parvulescu, S. Maurer, U. Muller, W.P. Zhang, Rare-earth ion exchanged Cu-SSZ-13 zeolite from organotemplate-free synthesis with enhanced hydrothermal stability in NH_3-SCR of NO_x, Catal. Sci. Technol. 9 (2019) 241–251, https://doi.org/10.1039/c8cy02033g.
[87] T. Fujiwara, H. Mori, Y. Mochizuki, H. Tatewaki, E. Miyoshi, Theoretical study of hydration models of trivalent rare-earth ions using model core potentials, J. Mol. Struct. -Theochem 949 (2010) 28–35, https://doi.org/10.1016/j.theochem.2010.02.032.
[88] P.S. Liu, Y. Cui, J.Y. Wang, X.H. Du, H.T. Zhang, A. Humphries, M.J. Jia, J.H. Yu, Structure stabilization of zeolite Y induced by yttrium and its role in promoting n-docosane conversion, Microporous Mesoporous Mat. 323 (2021) 111225, https://doi.org/10.1016/j.micromeso.2021.111225.
[89] G. Sun, R. Yu, L. Xu, B. Wang, W. Zhang, Enhanced hydrothermal stability and SO_2-tolerance of Cu–Fe modified AEI zeolite catalysts in NH_3-SCR of NO_x, Catal. Sci. Technol. 12 (2022) 3898–3911, https://doi.org/10.1039/d1cy02343h.
[90] F. Gao, Y. Zheng, R.K. Kukkadapu, Y.L. Wang, E.D. Walter, B. Schwenzer, J. Szanyi, C.H.F. Peden, Iron loading effects in Fe/SSZ-13 NH_3-SCR catalysts: nature of the Fe ions and structure-function relationships, ACS Catal. 6 (2016) 2939–2954, https://doi.org/10.1021/acscatal.6b00647.
[91] L. Kovarik, N.M. Washton, R. Kukkadapu, A. Devaraj, A.Y. Wang, Y.L. Wang, J. Szanyi, C.H.F. Peden, F. Gao, Transformation of active sites in Fe/SSZ-13 SCR catalysts during hydrothermal aging: a spectroscopic, microscopic, and kinetics study, ACS Catal. 7 (2017) 2458–2470, https://doi.org/10.1021/acscatal.6b03679.
[92] P. Hammershøi, Y. Jangjou, W.S. Epling, A.D. Jensen, T. Janssens, Reversible and irreversible deactivation of Cu-CHA NH_3-SCR catalysts by SO_2 and SO_3, Appl. Catal. B-Environ. 226 (2018) 38–45, https://doi.org/10.1016/j.apcatb.2017.12.018.
[93] J. Luo, D. Wang, A. Kumar, J. Li, K. Kamasamudram, N. Currier, A. Yezerets, Identification of two types of Cu sites in Cu/SSZ-13 and their unique responses to hydrothermal aging and sulfur poisoning, Catal. Today 267 (2016) 3–9, https://doi.org/10.1016/j.cattod.2015.12.002.
[94] Y.H. Li, W.Y. Song, J. Liu, Z. Zhao, M.L. Gao, Y.C. Wei, Q. Wang, J.L. Deng, The protection of CeO_2 thin film on Cu-SAPO-18 catalyst for highly stable catalytic NH_3-SCR performance, Chem. Eng. J. 330 (2017) 926–935, https://doi.org/10.1016/j.cej.2017.08.025.
[95] S. Ming, L. Pang, Z. Chen, Y. Guo, L. Guo, Q. Liu, P. Liu, Y. Dong, S. Zhang, T. Li, Insight into SO_2 poisoning over Cu-SAPO-18 used for NH_3-SCR, Microporous Mesoporous Mat 303 (2020) 110294, https://doi.org/10.1016/j.micromeso.2020.110294.
[96] Y.S. Cheng, C. Lambert, D.H. Kim, J.H. Kwak, S.J. Cho, C.H.F. Peden, The different impacts of SO_2 and SO_3 on Cu/zeolite SCR catalysts, Catal. Today 151 (2010) 266–270, https://doi.org/10.1016/j.cattod.2010.01.013.
[97] M.Q. Shen, Y. Zhang, J.Q. Wang, C. Wang, J. Wang, Nature of SO_3 poisoning on Cu/SAPO-34 SCR catalysts, J. Catal. 358 (2018) 277–286, https://doi.org/10.1016/j.jcat.2017.12.008.
[98] P.S. Hammershoi, Y. Jangjou, W.S. Epling, A.D. Jensen, T.V.W. Janssens, Reversible and irreversible deactivation of Cu-CHA NH_3-SCRcatalysts by SO_2 and SO_3, Appl. Catal. B-Environ. 226 (2018) 38–45, https://doi.org/10.1016/j.apcatb.2017.12.018.
[99] A. Kumar, M.A. Smith, K. Kamasamudram, N.W. Currier, H. An, A. Yezerets, Impact of different forms of feed sulfur on small-pore Cu-zeolite SCR catalyst, Catal. Today 231 (2014) 75–82, https://doi.org/10.1016/j.cattod.2013.12.038.
[100] L. Zhang, D. Wang, Y. Liu, K. Kamasamudram, J.H. Li, W. Epling, SO_2 poisoning impact on the NH_3-SCR reaction over a commercial Cu-SAPO-34 SCR catalyst, Appl. Catal. B-Environ. 156 (2014) 371–377, https://doi.org/10.1016/j.apcatb.2014.03.030.
[101] P.S. Hammershoi, P.N.R. Vennestrom, H. Falsig, A.D. Jensen, T.V.W. Janssens, Importance of the Cu oxidation state for the SO_2-poisoning of a Cu-SAPO-34 catalyst in the NH_3-SCR reaction, Appl. Catal. B-Environ. 236 (2018) 377–383, https://doi.org/10.1016/j.apcatb.2018.05.038.
[102] K. Wijayanti, K.P. Xie, A. Kumar, K. Kamasamudram, L. Olsson, Effect of gas compositions on SO_2 poisoning over Cu/SSZ-13 used for NH_3-SCR, Appl. Catal. B-Environ. 219 (2017) 142–154, https://doi.org/10.1016/j.apcatb.2017.07.017.
[103] P.S. Hammershoi, A.L. Godiksen, S. Mossin, P.N.R. Vennestrom, A.D. Jensen, T.V. W. Janssens, Site selective adsorption and relocation of SO_x in deactivation of Cu-CHA catalysts for NH_3-SCR, Reac. Chem. Eng. 4 (2019) 1081–1089, https://doi.org/10.1039/c8re00275d.
[104] J. Du, X. Shi, Y. Shan, G. Xu, Y. Sun, Y. Wang, Y. Yu, W. Shan, H. He, Effects of SO_2 on Cu-SSZ-39 catalyst for the selective catalytic reduction of NO_x with NH_3, Catal. Sci. Technol. 10 (2020) 1256–1263, https://doi.org/10.1039/c9cy02186h.
[105] M.Q. Shen, H.Y. Wen, T. Hao, T. Yu, D.Q. Fan, J. Wang, W. Li, J.Q. Wang, Deactivation mechanism of SO_2 on Cu/SAPO-34 NH_3-SCR catalysts: structure and active Cu^{2+}, Catal. Sci. Technol. 5 (2015) 1741–1749, https://doi.org/10.1039/c4cy01129e.
[106] K. Wijayanti, K. Leistner, S. Chand, A. Kumar, K. Kamasamudram, N.W. Currier, A. Yezerets, L. Olsson, Deactivation of Cu-SSZ-13 by SO_2 exposure under SCR conditions, Catal. Sci. Technol. 6 (2016) 2565–2579, https://doi.org/10.1039/c5cy01288k.
[107] A. Kumar, M.A. Smith, K. Kamasamudram, N.W. Currier, A. Yezerets, Chemical deSOx: an effective way to recover Cu-zeolite SCR catalysts from sulfur poisoning, Catal. Today 267 (2016) 10–16, https://doi.org/10.1016/j.cattod.2016.01.033.
[108] K.P. Xie, J. Woo, D. Bernin, A. Kumar, K. Kamasamudram, L. Olsson, Insights into hydrothermal aging of phosphorus-poisoned Cu-SSZ-13 for NH_3-SCR, Appl. Catal. B-Environ. 241 (2019) 205–216, https://doi.org/10.1016/j.apcatb.2018.08.082.
[109] J.L. Chen, Y.L. Shan, Y. Sun, W.Q. Ding, S. Xue, X.W. Han, J.P. Du, Z.D. Yan, Y. B. Yu, H. He, Hydrothermal aging alleviates the phosphorus poisoning of Cu- SSZ-39 catalysts for NH_3-SCR reaction, Environ. Sci. Technol. 57 (2023) 4113–4121, https://doi.org/10.1021/acs.est.2c08876.
[110] I. Lezcano-Gonzalez, U. Deka, D. Van, P. Paalanen, B. Arstad, B.M. Weckhuysen, A.M. Beale, Chemical deactivation of Cu-SSZ-13 ammonia selective catalytic reduction (NH_3-SCR) systems, Appl. Catal. B-Environ. 154–155 (2014) 339–349, https://doi.org/10.1016/j.apcatb.2014.02.037.
[111] P. Kern, M. Klimczak, T. Heinzelmann, M. Lucas, P. Claus, High-throughput study of the effects of inorganic additives and poisons on NH_3-SCR catalysts. Part II: Fe–zeolite catalysts, Appl. Catal. B-Environ. 95 (2010) 48–56, https://doi.org/10.1016/j.apcatb.2009.12.008.
[112] I. Lezcano-Gonzalez, U. Deka, H.E. van der Bij, P. Paalanen, B. Arstad, B. M. Weckhuysen, A.M. Beale, Chemical deactivation of Cu-SSZ-13 ammonia selective catalytic reduction (NH_3-SCR) systems, Appl. Catal. B-Environ. 154 (2014) 339–349, https://doi.org/10.1016/j.apcatb.2014.02.037.
[113] W. Kooten, H.C. Krijnsen, C. Bleek, H. Calis, Deactivation of zeolite catalysts used for NOx removal, Appl. Catal. B-Environ. 25 (2000) 125–135, https://doi.org/10.1016/S0926-3373(99)00125-3.
[114] P. Kern, M. Klimczak, T. Heinzelmann, M. Lucas, P. Claus, High-throughput study of the effects of inorganic additives and poisons on NH_3 -SCR catalysts. Part II: Fe–zeolite catalysts, Appl. Catal. B-Environ. 95 (2010) 48–56, https://doi.org/10.1038/jhh.2009.58.
[115] L. Wei, D.W. Yao, F. Wu, B. Liu, X.H. Hu, X.W. Li, X.L. Wang, Impact of hydrothermal aging on SO_2 poisoning over Cu-SSZ-13 diesel exhaust SCR catalysts, Ind. Eng. Chem. Res 58 (2019) 3949–3958, https://doi.org/10.1021/acs.iecr.8b04543.
[116] N. Zhu, W. Shan, Y. Shan, J. Du, Z. Lian, Y. Zhang, H. He, Effects of alkali and alkaline earth metals on Cu-SSZ-39 catalyst for the selective catalytic reduction of NO with NH_3, Chem. Eng. J. 388 (2020), https://doi.org/10.1016/j.cej.2020.124250.
[117] S. Ming, L. Pang, C. Fan, W. Guo, Y. Dong, P. Liu, Z. Chen, T. Li, Chemical deactivation of Cu-SAPO-18 deNO catalyst caused by basic inorganic contaminants in diesel exhaust, Chin. J. Catal. 40 (2019) 590–599, https://doi.org/10.1016/s1872-2067(19)63312-7.
[118] Q. Gao, Q. Ye, S. Han, H. Dai, Calcium poisoning mechanism of Cu-SAPO-18 for selective catalytic reduction of NO_x with ammonia, ChemistrySelect 5 (2020) 13477–13486, https://doi.org/10.1002/slct.202001604.
[119] L. Xie, F. Liu, L. Ren, X. Shi, F.S. Xiao, H. He, Excellent performance of One-Pot synthesized Cu-SSZ-13 catalyst for the selective catalytic reduction of NO_x with NH_3, Environ. Sci. Technol. 48 (2014) 566–572, https://doi.org/10.1021/es4032002.
[120] S. Han, J. Cheng, C. Zheng, Q. Ye, S. Cheng, T. Kang, H. Dai, Effect of Si/Al ratio on catalytic performance of hydrothermally aged Cu-SSZ-13 for the NH_3-SCR of NO in simulated diesel exhaust, Appl. Surf. Sci. 419 (2017) 382–392, https://doi.org/10.1016/j.apsusc.2017.04.198.
[121] Z. Zhao, R. Yu, R. Zhao, C. Shi, H. Gies, F.S. Xiao, D.D. Vos, T. Yokoi, X. Bao, U. Kolb, Cu-Exchanged Al-rich SSZ-13 zeolite from organotemplate-free synthesis as NH_3 -SCR catalyst: effects of Na^+ ions on the activity and hydrothermal stability, Appl. Catal. B-Environ. (2017) 421–428, https://doi.org/10.1016/j.apcatb.2017.06.013.
[122] J. Lee, J.R. Theis, E.A. Kyriakidou, Vehicle emissions trapping materials: successes, challenges, and the path forward, Appl. Catal. B-Environ. 243 (2019) 397–414, https://doi.org/10.1016/j.apcatb.2018.10.069.
[123] A. Westemann, B. Azambre, G. Finqueneisel, P. Da Costa, F. Can, Evolution of unburnt hydrocarbons under "cold-start" conditions from adsorption/desorption to conversion: On the screening of zeolitic materials, Appl. Catal. B-Environ. 158 (2014) 48–59, https://doi.org/10.1016/j.apcatb.2014.04.005.
[124] T. Zhang, F. Qiu, J. Li, Design and synthesis of core-shell structured meso-Cu-SSZ-13@mesoporous aluminosilicate catalyst for SCR of NO with NH_3: Enhancement of activity, hydrothermal stability and propene poisoning resistance, Appl. Catal. B-Environ. 195 (2016) 48–58, https://doi.org/10.1016/j.apcatb.2016.04.058.
[125] Q. Ye, L.F. Wang, R.T. Yang, Activity, propene poisoning resistance and hydrothermal stability of copper exchanged chabazite-like zeolite catalysts for SCR of NO with ammonia in comparison to Cu/ZSM-5, Appl. Catal. A-Gen. 427 (2012) 24–34, https://doi.org/10.1016/j.apcata.2012.03.026.

[126] J. Kim, Y. Kim, M.H. Wiebenga, S.H. Oh, D.H. Kim, Oxidation of C_3H_8, iso-C_5H_{12} and C_3H_6 under near-stoichiometric and fuel-lean conditions over aged Pt-Pd/Al_2O_3 catalysts with different Pt:Pd ratios, Appl. Catal. B-Environ. 251 (2019) 283–294, https://doi.org/10.1016/j.apcatb.2019.04.001.

[127] J. Kim, J. Shim, J.C. Kim, E. Jang, J.H. Lee, H. Baik, C.Y. Kang, C.H. Kim, K.-Y. Lee, S.K. Kwak, J. Choi, Unveiling the elusive roles of Cu species in determining the hydrocarbon trap performance during cold start in Cu-impregnated MFI type zeolites, Appl. Catal. B-Environ. 337 (2023), 122916, https://doi.org/10.1016/j.apcatb.2023.122916.

[128] Y.J. Kim, J.K. Lee, K.M. Min, S.B. Hong, I.S. Nam, B.K. Cho, Hydrothermal stability of Cu-SSZ-13 for reducing NO_x by NH_3, J. Catal. 311 (2014) 447–457, https://doi.org/10.1016/j.jcat.2013.12.012.

[129] S. Han, Q. Ye, S.Y. Cheng, T.F. Kang, H.X. Dai, Effect of the hydrothermal aging temperature and Cu/Al ratio on the hydrothermal stability of Cu-SSZ-13 catalysts for NH_3-SCR, Catal. Sci. Technol. 7 (2017) 703–717, https://doi.org/10.1039/c6cy02555b.

[130] J. Du, Y. Shan, Y. Sun, M. Gao, Z. Liu, X. Shi, Y. Yu, H. He, Unexpected increase in low-temperature NH_3-SCR catalytic activity over Cu-SSZ-39 after hydrothermal aging, Appl. Catal. B-Environ. 294 (2021), 120237, https://doi.org/10.1016/j.apcatb.2021.120237.